Moving solitons in the discrete nonlinear Schrödinger equation

O. F. Oxtoby[*] and I. V. Barashenkov[†]

Department of Maths and Applied Maths, University of Cape Town, Rondebosch 7701, South Africa

(Received 1 November 2006; revised manuscript received 17 July 2007; published 13 September 2007)

Using the method of asymptotics beyond all orders, we evaluate the amplitude of radiation from a moving small-amplitude soliton in the discrete nonlinear Schrödinger equation. When the nonlinearity is of the cubic type, this amplitude is shown to be nonzero for all velocities and therefore small-amplitude solitons moving without emitting radiation do not exist. In the case of a *saturable* nonlinearity, on the other hand, the radiation is found to be completely suppressed when the soliton moves at one of certain isolated "sliding velocities." We show that a discrete soliton moving at a general speed will experience radiative deceleration until it either stops and remains pinned to the lattice or—in the saturable case—locks, metastably, onto one of the sliding velocities. When the soliton's amplitude is small, however, this deceleration is extremely slow; hence, despite losing energy to radiation, the discrete soliton may spend an exponentially long time traveling with virtually unchanged amplitude and speed.

I. INTRODUCTION

This paper deals with moving solitons of the discrete non-linear Schrödinger (DNLS) equation. The earliest applications of the cubic DNLS equation were to the self-trapping of electrons in lattices (the polaron problem) and energy transfer in biological chains (Davydov solitons)—see the reviews in [1–3] for references. Relatedly, the equation arises in the description of small-amplitude breathers in Frenkel-Kontorova chains with weak coupling [1]. In optics the equation describes light-pulse propagation in nonlinear waveguide arrays in the tight-binding limit [4,5]. Most recently the DNLS has been used to model Bose-Einstein condensates in optically induced lattices [6].

The question of the existence of moving solitons in the DNLS equation has been the subject of debate for some time [7–19]. Recently, Gómez-Gardeñes *et al.* [20,21] have demonstrated that the stationary motion of pulses in the cubic one-site DNLS (the "standard" DNLS) is only possible over an oscillatory background consisting of a superposition of plane waves. This result was obtained by numerical continuation of the moving Ablowitz-Ladik breather with two commensurate time scales. In our present paper, we study the traveling discrete solitons analytically and independently of any reference models. Consistently with the conclusions of [20,21], we will show that solitons cannot freely move in the cubic DNLS equation; they emit radiation, decelerate, and eventually become pinned by the lattice. We shall show, however, that this radiation is exponentially small in the soliton's amplitude, so that broad, small-amplitude pulses are highly mobile and are for all practical purposes indistinguishable from freely moving solitons.

In the context of optical waveguide arrays—important not only in themselves but also as a first step to understanding more complicated optical systems such as photonic crystals—interest among experimentalists [22–24] has re-

cently shifted away from media with pure-Kerr nonlinearity (which gives rise to a cubic term in the DNLS equation) and towards photorefractive media, which exhibit a saturable nonlinearity [25–29]. In practice such arrays may be optically induced in a photorefractive material [22,23] or fabricated permanently—see [24], for example. The study of solitons in *continuous* optical systems with saturable nonlinearitites has a long history; interesting phenomena here include bistability [30,31], fusion [32], and radiation effects [33] which do not arise in the cubic equation. As for the *discrete* case, the work of Khare *et al.* [34] suggests that the saturable one-site DNLS may be *exceptional* in the sense of Ref. [35]; that is, despite not being a translation invariant system, it supports translationally invariant stationary solitons. This property is usually seen as a prerequisite for undamped motion in discrete equations (see, e.g., [36]), and indeed, the numerical experiments of Vicencio and Johansson [29] have revealed that soliton mobility is enhanced in the saturable DNLS equation.

The DNLS equation with a saturable nonlinearity is the second object of our analysis here; our conclusions will turn out to be in agreement with the numerical observations of Ref. [29]. We will show that for nonlinearities which saturate at a low enough intensity, solitons can *slide*—that is, move without radiative deceleration—at certain isolated velocities. These "sliding" solitons are examples of embedded solitons.

The usual saturable DNLS equation is the discrete form of the Vinetskii-Kukhtarev model [37]:

$$i\dot{\Phi}_n + \Phi_{n+1} - 2\Phi_n + \Phi_{n-1} - \gamma \frac{1}{1+|\Phi_n|^2}\Phi_n = 0. \quad (1)$$

In order to encompass both cubic and saturable nonlinearities in a single model, we shall instead consider the equation

$$i\dot{\phi}_n + \phi_{n+1} + \phi_{n-1} + \frac{2|\phi_n|^2}{1+\mu|\phi_n|^2}\phi_n = 0, \quad (2)$$

obtained from Eq. (1) by making the transformation $\Phi_n = \sqrt{2/\gamma}\, e^{-i(2+\gamma)t}\phi_n$ and letting $\mu = 2/\gamma$. In the form above, $1/\mu$ represents the saturation threshold of the medium [31],

*Oliver.Oxtoby@uct.ac.za

†Igor.Barashenkov@uct.ac.za; igor@odette.mth.uct.ac.za

which tends to infinity as one approaches the pure Kerr (cubic) case of $\mu = 0$. The higher the value of μ, the lower is the intensity at which the nonlinearity saturates.

This paper is structured in the following way. In Sec. II, we construct a small-amplitude, broad traveling pulse as an asymptotic series in powers of ϵ, its amplitude. The velocity and frequency of this soliton are obtained as explicit functions of ϵ and its carrier-wave wavenumber. Then in Sec. III, the main section of this paper, we derive an expression for the soliton's radiation tails and measure their amplitude using the method of asymptotics beyond all orders. In Sec. IV, we investigate the influence of this exponentially weak radiation on the soliton's amplitude and speed. Finally, in Sec. V, we summarize our work and make comparisons with some earlier results.

II. ASYMPTOTIC EXPANSION

A. Leading order

We begin by seeking solutions of the form

$$\phi_n(t) = \psi(X)e^{ikn+i\omega t}, \tag{3}$$

where

$$X = \epsilon(n - vt) \tag{4}$$

and ϵ is a parameter. By analogy with the soliton of the continuous NLS equation, we expect the discrete soliton to be uniquely characterized by two parameters—e.g., ϵ and k—while the other two (ω and v) are expected to be expressible through ϵ and k. Substituting the ansatz (3) with Eq. (4) into Eq. (2) gives a differential advance-delay equation

$$\psi(X+\epsilon)e^{ik} + \psi(X-\epsilon)e^{-ik} - \omega\psi(X) - i\epsilon v\psi'(X)$$
$$+ \frac{2|\psi(X)|^2}{1+\mu|\psi(X)|^2}\psi(X) = 0. \tag{5}$$

This can be written as an ordinary differential equation of an infinite order:

$$e^{ik}\sum_{n=0}^{\infty}\epsilon^n\frac{1}{n!}\psi^{(n)} + e^{-ik}\sum_{n=0}^{\infty}\epsilon^n\frac{(-1)^n}{n!}\psi^{(n)} - \omega\psi - i\epsilon v\psi'$$
$$+ \frac{2|\psi|^2}{1+\mu|\psi|^2}\psi = 0, \tag{6}$$

where $\psi^{(n)} = d^n\psi/dX^n$.

From now on we assume that ϵ is small. Our aim in this section is to find an approximate solution to Eq. (6)—and hence Eq. (2)—with $\psi = O(\epsilon)$. (That is, we are looking for small, broad pulses which modulate a periodic carrier wave.) To this end, we expand ψ, ω, and v as power series in ϵ:

$$\psi = \epsilon(\psi_0 + \epsilon\psi_1 + \cdots), \tag{7a}$$

$$\omega = \omega_0 + \epsilon^2\omega_2 + \cdots, \tag{7b}$$

$$v = v_0 + \epsilon^2 v_2 + \cdots. \tag{7c}$$

(We are not expanding k as we consider it, along with ϵ, as one of the two independent parameters characterizing our

solution.) Substituting these expansions into Eq. (6) gives a hierarchy of equations to be satisfied at each power of ϵ by choosing ω_n and v_n properly. In nonlinear oscillations, this perturbation procedure is known as Lindstedt's method [38].

At the order ϵ^1 we obtain

$$\omega_0 = 2\cos k, \tag{8}$$

while the order ϵ^2 gives

$$v_0 = 2\sin k. \tag{9}$$

These two relations correspond to the dispersion of linear waves. At the power ϵ^3 we obtain the following nonlinear equation for ψ_0:

$$\cos k\,\psi_0'' - \omega_2\psi_0 + 2|\psi_0|^2\psi_0 = 0.$$

This is the stationary form of the NLS equation, which has the homoclinic solution

$$\psi_0 = a\sqrt{\cos k}\,\text{sech}(aX),$$

with

$$a^2 = \frac{\omega_2}{\cos k}.$$

Returning to the original variable ψ, we note that the amplitude a can always be absorbed into ϵ, the parameter in Eq. (4), and in front of ψ_0 in Eq. (7a). That is, there is no loss of generality in setting $a = 1$ and letting ϵ describe the amplitude (and inverse width) of the pulse instead. This allows us to set

$$\omega_2 = \cos k. \tag{10}$$

Note that the coefficients in Eq. (5) are periodic functions of the parameter k with period 2π; therefore, it is sufficient to consider k in the interval $(-\pi, \pi)$. Also, Eq. (5) is invariant with respect to the transformation $k \to -k$, $\epsilon \to -\epsilon$, $v \to -v$; hence, it is sufficient to consider positive k only. Finally, our perturbative solution does not exist if $\cos k$ is negative. Thus, from now on we shall assume that $0 \leq k \leq \pi/2$.

B. Higher orders

At the order ϵ^{n+3}, where $n \geq 1$, we arrive at the following equations for the real and imaginary parts of ψ_n:

$$\mathcal{L}_1\,\text{Re}\,\psi_n = \frac{\text{Re}\,f_{n-1}(X)}{\cos k}, \tag{11a}$$

$$\mathcal{L}_0\,\text{Im}\,\psi_n = \frac{\text{Im}\,f_{n-1}(X)}{\cos k}, \tag{11b}$$

where

$$\mathcal{L}_0 = -d^2/dX^2 + 1 - 2\,\text{sech}^2 X,$$

$$\mathcal{L}_1 = -d^2/dX^2 + 1 - 6\,\text{sech}^2 X,$$

and

$$f_{n-1}(X) = \sum_{j=1}^{[n/2]} \left(\frac{2\cos k}{(2j+2)!} \psi_{n-2j}^{(2j+2)} - \omega_{2j+2}\psi_{n-2j} \right) + i \sum_{j=1}^{[(n+1)/2]} \left(\frac{2\sin k}{(2j+1)!} \psi_{n-2j+1}^{(2j+1)} - v_{2j}\psi'_{n-2j+1} \right) + \sum_{m=1}^{n-1} 2\psi_0(\psi_m\psi_{n-m}^* - \psi_{n-m}\psi_m^*)$$

$$+ \sum_{m=1}^{n-1}\sum_{\ell=0}^{n-1-m} 2\psi_{n-m-\ell}\psi_m\psi_\ell^* + \mu \sum_{m=0}^{n-1}\sum_{\ell=0}^{n-1-m} \left[\sum_{j=1}^{[(n-m-\ell)/2]} \left(\frac{2\cos k}{(2j)!} \psi_{n-m-\ell-2j}^{(2j)} - \omega_{2j}\psi_{n-m-\ell-2j} \right) \right.$$

$$+ i \sum_{j=1}^{[(n-m-\ell-1)/2]} \left. \left(\frac{2\sin k}{(2j+1)!} \psi_{n-m-\ell-2j-1}^{(2j+1)} - v_{2j}\psi'_{n-m-\ell-2j-1} \right) \right] \psi_m\psi_\ell^*. \tag{12}$$

The linear nonhomogeneous ordinary differential equations (11) must be solved subject to a boundedness condition.

The bounded homogeneous solutions of Eqs. (11a) and (11b) (sech X tanh X and sech X, respectively) correspond to the translation and U(1) invariances of Eq. (5). Including these zero modes in the full solution of Eqs. (11) would amount just to the translation of $\psi(X)$ by a constant distance in X and its multiplication by a constant phase factor. These deformations are trivial, and hence we can safely discard the homogeneous solutions at each order of ϵ.

As ψ_0's real part is even and its imaginary part is odd (zero), ψ_1's real and imaginary parts are also even and odd, respectively. The same holds, by induction, to all orders of the perturbation theory. Indeed, assume that $\psi_0, \psi_1, \ldots, \psi_{n-1}$ have even real parts and odd imaginary parts. Then it is not difficult to verify that the function Re $f_{n-1}(X)$ is even and Im $f_{n-1}(X)$ is odd. Since the operators $\mathcal{L}_0$ and $\mathcal{L}_1$ are parity preserving and since we have excluded the corresponding homogeneous solutions, this means that ψ_n has an even real part and an odd imaginary part. Finally, the homogeneous solution of Eq. (11b) being even and that of Eq. (11a) being odd, the corresponding solvability conditions are satisfied at any order.

Note that since the solvability conditions do not impose any constraints on v_n and ω_n, the coefficients v_n with $n \geq 2$ and ω_n with $n \geq 4$ can be chosen completely arbitrarily.

C. Explicit perturbative solution to order ϵ^3

Solving Eqs. (11) successively, we can obtain the discrete soliton (7a) to any desired accuracy. Here, we restrict ourselves to corrections up to the cubic power in ϵ. The order ϵ^3 is the lowest order at which the saturation parameter μ appears in the solution. On the other hand, it is high enough to exemplify and motivate our choice of the coefficients in Eqs. (7b) and (7c).

Letting $n=1$ in Eq. (12), we have

$$f_0(X) = \frac{2i}{3!}\sin k\,\psi_0''' - iv_2\psi_0'.$$

The corresponding solution of Eq. (11) is

$$\psi_1 = \frac{i}{\sqrt{\cos k}}\left[\frac{1}{2}\sin k\,\text{sech}\,X\,\text{tanh}\,X \right.$$

$$\left. + \frac{1}{2}\left(v_2 - \frac{1}{3}\sin k \right)X\,\text{sech}\,X \right].$$

Here the term proportional to X sech X decays to zero as $|X| \to \infty$; however, it becomes greater than $\psi_0(X)$ for sufficiently large $|X|$, leading to nonuniformity of the expansion (7a). In order to obtain a uniform expansion, the term in question should be eliminated. Being free to choose the coefficients v_n with $n \geq 2$, we use this freedom to set

$$v_2 = \frac{1}{3}\sin k.$$

This leaves us with

$$\psi_1 = \frac{i}{2}\sqrt{\cos k}\,\tan k\,\text{sech}\,X\,\text{tanh}\,X.$$

After "distilling" in a similar way the correction ψ_2, where we fix

$$\omega_4 = \frac{1}{12}\cos k$$

to eliminate a term proportional to X sech X, we obtain

$$\psi = \epsilon\sqrt{\cos k}\left\{ \text{sech}\,X + \frac{i}{2}\epsilon\tan k\,\text{sech}\,X\,\text{tanh}\,X \right.$$

$$+ \frac{1}{12}\epsilon^2\left[4\,\text{sech}^3\,X - 3\,\text{sech}\,X + \frac{1}{2}\tan^2 k(14\,\text{sech}^3\,X \right.$$

$$\left. - 13\,\text{sech}\,X) + 4\mu\cos k(2\,\text{sech}\,X - \text{sech}^3\,X) \right] + O(\epsilon^3) \Bigg\},$$

$$\tag{13}$$

where

$$\omega = 2\left[1 + \frac{1}{2!}\epsilon^2 + \frac{1}{4!}\epsilon^4 + O(\epsilon^6) \right]\cos k, \tag{14a}$$

$$v = 2\left[1 + \frac{1}{3!}\epsilon^2 + O(\epsilon^4) \right]\sin k. \tag{14b}$$

D. Velocity and frequency of the discrete soliton

In the previous subsection we have shown that fixing suitably the coefficients ω_n and v_n can lead to a uniform expansion of ψ to order ϵ^3. Our approach was based on solving for ψ_n explicitly and then setting the coefficients in front of the "secular" terms $X \operatorname{sech} X$ to zero. Here, we show that the secular terms can be eliminated to all orders—and without appealing to explicit solutions.

Assume that the secular terms have been suppressed in all nonhomogeneous solutions ψ_m with m up to $n-1$; that is, let

$$\psi_m(X) \to C_m e^X + o(e^X) \quad \text{as } X \to -\infty$$

$$(m = 0, 1, \ldots, n-1). \tag{15}$$

(Since we know that the real part of ψ_m is even and the imaginary part odd, it is sufficient to consider the asymptotic behavior at one infinity only.) The constant C_m may happen to be zero for some m in which case the decay of ψ_m will be faster than e^X. Our objective is to choose ω_n and v_n in such a way that $\psi_n(X)$ will also satisfy (15). To this end, we consider the function (12). All terms which are trilinear in $\psi_0, \ldots, \psi_{n-1}$ and derivatives of these functions decay as e^{3X} or faster; these terms in f_{n-1} cannot give rise to the secular terms proportional to $X \operatorname{sech} X$ in ψ_n. On the other hand, the terms making up the first line in (12) tend to

$$e^X \sum_{j=1}^{[n/2]} \left[\frac{2\cos k}{(2j+2)!} - \omega_{2j+2} \right] C_{n-2j}$$

$$+ ie^X \sum_{j=1}^{[(n+1/2)]} \left[\frac{2\sin k}{(2j+1)!} - v_{2j} \right] C_{n-2j+1}$$

as $X \to -\infty$. These are "asymptotically resonant" terms—in the sense that their asymptotics are proportional to the asymptotics of the homogeneous solutions of Eqs. (11a) and (11b). It is these terms on the right-hand sides of Eqs. (11a) and (11b) that give rise to the secular terms in the solution ψ_n. The resonant terms will be suppressed if we let

$$\omega_{2j+2} = \frac{2\cos k}{(2j+2)!}, \quad v_{2j} = \frac{2\sin k}{(2j+1)!}, \quad j \geq 1. \tag{16}$$

After the resonant terms have been eliminated, the bounded solution to Eqs. (11) will have the asymptotic behavior $\psi_n \to C_n e^X$ as $X \to -\infty$. By induction, this result extends to all $n \geq 0$.

Substituting Eqs. (16), together with Eqs. (8)–(10), into Eqs. (7b) and (7c), and summing up the series, we obtain

$$\omega = 2\cos k \cosh \epsilon, \quad v = 2\sin k \frac{\sinh \epsilon}{\epsilon}, \tag{17}$$

the frequency and velocity of the discrete soliton parametrized in terms of k and ϵ.

Equations (17) coincide with the expressions [39] of the Ablowitz-Ladik soliton's velocity and frequency in terms of its amplitude and wavenumber. The difference between the two sets of answers is in that Eqs. (17) pertain to small-amplitude solitons only, whereas Ablowitz and Ladik's formulas are valid for arbitrarily large amplitudes.

Note, also, that the velocity and frequency (17) do not depend on the saturation parameter μ. This is in contrast to the stationary ($v=0$) soliton of Eqs. (5) and (6) obtained by Khare *et al.* [34]. The soliton of Ref. [34] has its amplitude and frequency uniquely determined by μ.

III. TERMS BEYOND ALL ORDERS OF THE PERTURBATION THEORY

A. Dispersion relation for linear waves

As $X \to -\infty$, the series (7a) reduces to $\psi(X) = \sum_{n=0}^{\infty} \epsilon^{n+1} C_n e^X$. The convergence of the series $\sum \epsilon^{n+1} \psi_n(X)$ for all X would imply, in particular, the convergence of the series $\sum \epsilon^{n+1} C_n$. Therefore, if the series (7a) converged, the solution $\psi(X)$ would be decaying to zero as $X \to -\infty$. However, although we have shown that the series $\sum \epsilon^{n+1} \psi_n(X)$ is asymptotic to all orders, it does not have to be convergent. For instance, it is easy to see that the series cannot converge for $v=\mu=0$ and any ϵ; since the advance-delay equation (5) is translation invariant, this would imply that we have constructed a family of stationary solitons with an arbitrary position relative to the lattice. This, in turn, would contradict the well-established fact that the "standard" cubic DNLS solitons can only be centered on a site or midway between two adjacent sites [40] (that is, that the "standard" discretization of the cubic NLS equation is not exceptional [41]). Thus, we expect that the perturbative solution (7a) satisfies $\psi(X) \to 0$ as $|X| \to \infty$ only for some special choices of v, ϵ, and μ.

Can Eqs. (5) and (6) have a bounded solution despite the divergence of the corresponding series $\sum \epsilon^{n+1} C_n$? To gain some insight into this matter, we linearize Eq. (5) about $\psi = 0$ and find nondecaying solutions of the form $\psi = e^{i\mathcal{Q}X/\epsilon}$ where $\mathcal{Q}$ is a root of the dispersion relation

$$\omega = 2\cos(k + \mathcal{Q}) + \mathcal{Q}v. \tag{18}$$

It is easy to check that there is at least one such harmonic solution [i.e., Eq. (18) has at least one root] if $v \neq 0$. These harmonic waves can form a radiation background over which the soliton propagates (as suggested by the numerics of [20,21] and the analysis of a similar problem for the ϕ^4 kinks in [36]). Being nonanalytic in ϵ, such backgrounds cannot be captured by any order of the perturbation expansion.

As we will show below, not only the wavenumbers but also the amplitudes of the harmonic waves are nonanalytic in ϵ. This phenomenon was first encountered in the context of the breather of the continuous ϕ^4 model, where Eleonskii *et al.* [42] suggested that the radiation from the breather could be exponentially weak. Segur and Kruskal [43,44] then developed the method of "asymptotics beyond all orders" to demonstrate that, in the limit $\epsilon \to 0$, such radiation does exist. We will use Segur and Kruskal's method to measure the magnitude of the radiation background of the traveling discrete soliton.

Qualitatively, the fact that the radiation is not excited at any order of the perturbation expansion is explained by the fact that the soliton exists on the long length scale X, whereas the radiation has the shorter scale X/ϵ. To all orders, the two are uncoupled.
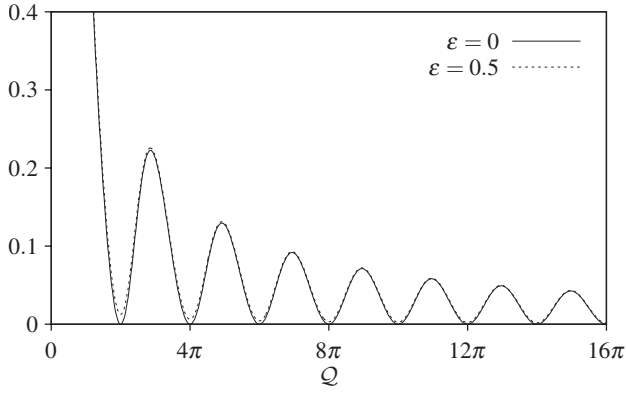
FIG. 1. The left-hand side of Eq. (19) for two values of ϵ. The root(s) $\mathcal{Q}_n$ of the dispersion relation (18) are located where this graph is intersected by a horizontal straight line with ordinate equal to $\tan k$.

Using the relations (17), we can rewrite Eq. (18) as

$$\frac{\cosh \epsilon - \cos \mathcal{Q}}{(\sinh \epsilon / \epsilon)\mathcal{Q} - \sin \mathcal{Q}} = \tan k. \qquad (19)$$

The left-hand side is plotted in Fig. 1. For $\epsilon = 0$ it has minima at multiples of 2π where the curve is tangent to the horizontal axis. For nonzero ϵ, the minima of the curve are lifted off the $\mathcal{Q}$ axis slightly. The minima with larger values of $\mathcal{Q}$ have smaller elevations above the horizontal axis; i.e., the minima come closer and closer to the $\mathcal{Q}$ axis as $\mathcal{Q}$ grows. We see from the figure that for $k > k_{max}^{(1)}$, where $k_{max}^{(1)} \approx 0.22$, there is only one radiation mode. Note also that the left-hand side of Eq. (19) is negative for negative $\mathcal{Q}$; since we have assumed that $0 \leqslant k \leqslant \pi/2$, this implies that Eq. (19) cannot have negative roots.

B. Radiating solitons

Although we originally constructed the expansion (7a) as an asymptotic approximation to a solution which is stationary in the frame of reference moving with the velocity v, it can also represent an approximation to a time-dependent solution $\psi(X,t)$. Here $\psi(X,t)$ is related to $\phi_n(t)$, the discrete variable in Eq. (2), by the substitution (3):

$$\phi_n(t) = \psi(X,t)e^{ikn+i\omega t}. \qquad (20)$$

The coefficients ψ_n in the asymptotic expansion of $\psi(X,t)$ will coincide with the coefficients in the expansion of the stationary solution $\psi(X) = \Sigma \epsilon^{n+1}\psi_n$ if the time derivatives $\partial_t \psi_n$ lie beyond all orders of ϵ and hence the time evolution of the free parameters k and ϵ occurs on a time scale longer than any power of ϵ^{-1}. Physically, one such solution represents a traveling soliton slowing down and attenuating as the Cherenkov radiation left in its wake carries momentum and energy away from its core.

Substituting Eq. (20) into Eq. (2), gives

$$i\psi_t + \psi^+ e^{ik} + \psi^- e^{-ik} - \omega\psi - i\epsilon v \psi_X + \frac{2|\psi|^2}{1 + \mu|\psi|^2}\psi = 0, \qquad (21)$$

where $\psi^{\pm} = \psi(X \pm \epsilon, t)$.

We consider two solutions of this equation which both have the same asymptotic expansion (7a), denoted $\psi_s(X,t)$ and $\psi_u(X,t)$, such that $\psi_s(X,t) \to 0$ as $X \to +\infty$ and $\psi_u(X,t) \to 0$ as $X \to -\infty$. Since the difference $\Psi \equiv \psi_s - \psi_u$ is small (lies beyond all orders of ϵ) and since the solution ψ_s can be regarded as a perturbation of ψ_u, Ψ obeys the linearization of Eq. (21) about ψ_u to a good approximation—that is,

$$i\Psi_t + \Psi^+ e^{ik} + \Psi^- e^{-ik} - \omega\Psi - iv\epsilon\Psi_X + \frac{4|\psi_u|^2\Psi + 2\psi_u^2\Psi^*}{1 + \mu|\psi_u|^2}$$
$$+ \frac{2\mu|\psi_u|^2(|\psi_u|^2\Psi + \psi_u^2\Psi^*)}{(1 + \mu|\psi_u|^2)^2} = 0. \qquad (22)$$

Since $\psi_u = O(\epsilon)$, we can solve Eq. (22) to leading order in ϵ by ignoring the last two terms in it; the resulting solutions are exponentials of the form $e^{i\mathcal{Q}X/\epsilon - i\Omega t}$. We make a preemptive simplification by setting $\Omega = 0$. [That Ω has to be set equal to zero follows from matching these exponentials to the far-field asymptotes of the stationary "inner" solution; see Sec. III D below. Physically, $\Omega = 0$ implies that the traveling pulse will only excite the radiation with its own (zero) frequency in the comoving frame.] The leading-order solution of Eq. (22) is therefore

$$\Psi = \sum_n A_n e^{i\mathcal{Q}_n X/\epsilon} + O(\epsilon^1), \qquad (23)$$

where $\mathcal{Q}_n$ ($n = 1, 2, \dots$) are the roots, numbered in order from smallest to largest, of the dispersion relation (18). (Recall that since we have taken k in the interval $[0, \pi/2]$, all the roots $\mathcal{Q}_n$ are positive.) For $k > k_{max}^{(1)} \approx 0.22$, there is only one root, $\mathcal{Q}_1$.

Higher-order corrections to the solution (23) can be found by substituting the ansatz

$$\Psi = \sum_n A_n [1 + \epsilon f_1^{(n)}(X) + \epsilon^2 f_2^{(n)}(X) + \cdots] e^{i\mathcal{Q}_n X/\epsilon}$$
$$+ \sum_n A_n^* [\epsilon^2 g_2^{(n)}(X) + \epsilon^3 g_3^{(n)}(X) + \cdots] e^{-i\mathcal{Q}_n X/\epsilon} \quad (24)$$

into Eq. (22), expanding the advance and delay terms $f_{1,2,\dots}^{(n)}(X \pm \epsilon)$, $g_{2,3,\dots}^{(n)}(X \pm \epsilon)$ in Taylor series in ϵ, and making use of the asymptotic expansion (13) for ψ_u. For instance, the first few corrections are found to be

$$f_1^{(n)}(X) = \frac{4i \cos k}{2 \sin(k + \mathcal{Q}_n) - v} \tanh X,$$

$$g_2^{(n)}(X) = \frac{2 \cos k}{\omega + vq_n - 2\cos(k - \mathcal{Q}_n)} \operatorname{sech}^2 X. \qquad (25)$$

Since $\psi_u \to 0$ as $X \to -\infty$, it follows that $\psi_s \to \Psi$ as $X \to -\infty$, and hence, once we know the amplitudes A_n, we know the asymptotic behavior of ψ_s. We shall now employ the

method of asymptotics beyond all orders to evaluate these amplitudes.

C. "Inner" equations

Segur and Kruskal's method allows one to measure the amplitude of the exponentially small radiation by continuing the solution analytically into the complex plane. The leading-order term of ψ, $\epsilon\sqrt{\cos k} \operatorname{sech} X$, has singularities at $X = \frac{i\pi}{2} + i\pi n$, $n = 0, \pm 1, \pm 2, \ldots$. In the vicinity of these points, the radiation becomes significant; the qualitative explanation for this is that the sech function forms a sharp spike with a short length scale near the singularity point, and hence there is a strong coupling to the radiation modes, unlike on the real axis. The radiation, which is exponentially small on the real axis, becomes large enough to be measured near the singularities.

We define a new complex variable y, such that ϵy is small in absolute value when X is near the lowest singularity in the upper half-plane:

$$\epsilon y = X - \frac{i\pi}{2}. \tag{26}$$

The variables y and X are usually referred to as the "inner" and "outer" variables, respectively—the transformation to y effectively "zooms in" on the singularity at $X = \frac{i\pi}{2}$. We also define $u(y) \equiv \psi(X)$ and $w(y) \equiv \psi^*(X)$. Continuing Eq. (5) to the complex plane—i.e., substituting $u(y)$ for $\psi(X)$ and $w(y)$ for $\psi^*(X)$—we obtain, in the limit $\epsilon \to 0$,

$$e^{ik}u(y+1) + e^{-ik}u(y-1) - 2\cos k\, u(y) - 2i\sin k\, u'(y)$$
$$+ \frac{2u^2 w}{1 + \mu uw} = 0, \tag{27a}$$

$$e^{-ik}w(y+1) + e^{ik}w(y-1) - 2\cos k\, w(y) + 2i\sin k\, w'(y)$$
$$+ \frac{2w^2 u}{1 + \mu wu} = 0. \tag{27b}$$

Here we have used the fact that $\omega \to 2\cos k$ and $v \to 2\sin k$ as $\epsilon \to 0$. Equations (27) are our "inner equations"; they are valid in the "inner region" $-\infty < \operatorname{Re} y < \infty$, $\operatorname{Im} y < 0$. (The solution cannot be continued up from the real X axis past the singularity at $y = 0$.)

Solving the system (27) order by order, we can find solutions in the form of a series in powers of y^{-1}. Alternatively, we can make the change of variables (26) in the asymptotic expansion (13) and send $\epsilon \to 0$. This gives, for the first few terms,

$$\hat{u} = \sqrt{\cos k}\left\{ -\frac{i}{y} + \tan k \frac{1}{2y^2} \right.$$
$$\left. + \left[\frac{1}{3}(1 - \mu\cos k) + \frac{7}{12}\tan^2 k \right]\frac{i}{y^3} + O(y^{-4}) \right\}, \tag{28a}$$

$$\hat{w} = \sqrt{\cos k}\left\{ -\frac{i}{y} - \tan k \frac{1}{2y^2} \right.$$
$$\left. + \left[\frac{1}{3}(1 - \mu\cos k) + \frac{7}{12}\tan^2 k \right]\frac{i}{y^3} + O(y^{-4}) \right\}. \tag{28b}$$

We are using carets over u and w to distinguish the series solution (28) from other solutions of Eq. (27) that will appear in the next section. The asymptotic series (28) may or may not converge. We note a symmetry $\hat{u}(-y) = -\hat{w}(y)$ of the power-series solution.

D. Exponential expansion

In order to obtain an expression for the terms which lie beyond all orders of y^{-1}, we substitute $(u, w) = (\hat{u}, \hat{w}) + (\delta u, \delta w)$ into Eqs. (27). Since $\hat{u}$ and $\hat{w}$ solve the equations to all orders in y^{-1}, then provided δu and δw are small, they will solve the linearization of Eqs. (27) about $(\hat{u}, \hat{w})$ for large $|y|$.

Formal solutions to the linearized system can be constructed as series in powers of y^{-1}. Because $\hat{u}$ and $\hat{w}$ are both $O(y^{-1})$, the leading-order expressions for δu and δw as $y \to \infty$ are obtained by substituting zero for $\hat{u}$ and $\hat{w}$ in the linearized equations. This gives

$$\delta u \to \sum_n J_n \exp(iq_n y),$$

$$\delta w \to \sum_n K_n \exp(-iq_n y) \quad \text{as } y \to \infty, \tag{29}$$

where q_n $(n = 0, 1, 2, \ldots)$. are the roots of

$$\cos(k + q) - \cos k + q\sin k = 0. \tag{30}$$

Note that the roots q_n with $n \geq 1$ are given by the $\epsilon \to 0$ limits of the roots of the dispersion equation (19): $q_n = \lim_{\epsilon \to 0} \mathcal{Q}_n$. In addition, there is a root $q_0 = 0$ which does not have a $\mathcal{Q}_0$ counterpart.

The full solutions (i.e., solutions including corrections to all orders in y^{-1}) will result if we use the full inverse-power series (28) for $\hat{u}$ and $\hat{w}$; these solutions should have the form

$$\delta u = \sum_n K_n \sum_{m=1}^{\infty} \frac{d_m^{(n)}}{y^m} \exp(-iq_n y), \tag{31a}$$

$$\delta w = \sum_n K_n \left[1 + \sum_{m=1}^{\infty} \frac{c_m^{(n)}}{y^m} \right] \exp(-iq_n y). \tag{31b}$$

Note that we have excluded the terms proportional to $e^{iq_n y}$ from this ansatz (i.e., set the amplitudes J_n to zero) as they would become exponentially large on the real X axis. [One can readily verify this by making the change of variables (26) in Eq. (29).] The coefficients $c_1^{(n)}, c_2^{(n)}, \ldots$ and $d_1^{(n)}, d_2^{(n)}, \ldots$ are found recursively when the ansatz (31) is substituted into the linearized equations and like powers of y^{-1} collected. In particular, the first few coefficients are

$$c_1^{(n)} = - \frac{2i \cos k}{\sin(k + q_n) - \sin k},$$

$$c_2^{(n)} = \frac{[\cos(k + q_n) - 2 \cos k] \cos k}{[\sin(k + q_n) - \sin k]^2} \quad (32a)$$

and

$$d_1^{(n)} = 0, \quad d_2^{(n)} = \frac{\cos k}{\cos(k - q_n) - \cos k - q_n \sin k}, \quad (32b)$$

where $n = 1, 2, \ldots$.

Having restricted ourselves to considering the linearized equations for δu and δw, we have only taken into account the simple harmonics in Eqs. (29) and (31). Writing $\delta u = \varepsilon^1 U_1 + \varepsilon^2 U_2 + \cdots$. and $\delta w = \varepsilon^1 W_1 + \varepsilon^2 W_2 + \cdots$, where ε is an auxiliary small parameter (not to be confused with our "principal" small parameter ϵ), substituting $u = \hat{u} + \delta u$ and $w = \hat{w} + \delta w$ in Eqs. (27), and solving order-by-order the resulting hierarchy of nonhomogeneous linear equations, we can recover all nonlinear corrections to δu and δw. The ε^2 corrections will be proportional to $e^{-i(q_n + q_m)y}$; higher-order corrections will introduce harmonics with higher combination wavenumbers. Later in this section it will become clear that ε is actually of

the order $\exp(-\pi \mathcal{Q}_1/2\epsilon)$ [see Eq. (36) below]; hence, the amplitudes of the combination harmonics will be exponentially smaller than that of $\exp(-iq_1 y)$.

Now we return to the object that is of ultimate interest to us in this work—that is, to the function Ψ of Sec. III B representing the radiation of the moving soliton. We need to match Ψ to the corresponding object in the inner region. To this end, we recall that $\Psi = \psi_s - \psi_u$, where ψ_s and ψ_u are two solutions of the outer equation (5) which share the same asymptotic expansion to all orders. In the limit $\epsilon \to 0$, the corresponding functions

$$u_s(y,t) \equiv \psi_s(X,t), \quad w_s(y,t) \equiv \psi_s^*(X,t),$$

$$u_u(y,t) \equiv \psi_u(X,t), \quad w_u(y,t) \equiv \psi_u^*(X,t) \quad (33)$$

solve Eqs. (27) and share the same inverse-power expansions. We express this fact by writing

$$u_s(y,t) \sim \hat{u}(y), \quad w_s(y,t) \sim \hat{w}(y),$$

$$u_u(y,t) \sim \hat{u}(y), \quad w_u(y,t) \sim \hat{w}(y).$$

Therefore, the difference $u_s - u_u$ (which results from the analytic continuation of the function Ψ) can be identified with δu and $w_s - w_u$ with δw. Continuing Eq. (24) and its complex conjugate gives, as $\epsilon \to 0$,

$$u_s - u_u = \sum_n \lim_{\epsilon \to 0} A_n(\epsilon) \exp\left(-\frac{\pi \mathcal{Q}_n}{2\epsilon}\right) \left[1 + O\left(\frac{1}{y}\right)\right] \exp(iq_n y)$$

$$- \sum_n \lim_{\epsilon \to 0} A_n^*(\epsilon) \exp\left(\frac{\pi \mathcal{Q}_n}{2\epsilon}\right) \left[\frac{2 \cos k}{\omega + vq_n - 2\cos(k - q_n)} \frac{1}{y^2} + O\left(\frac{1}{y^3}\right)\right] \exp(-iq_n y) \quad (34a)$$

and

$$w_s - w_u = \sum_n \lim_{\epsilon \to 0} A_n^*(\epsilon) \exp\left(\frac{\pi \mathcal{Q}_n}{2\epsilon}\right) \left[1 + O\left(\frac{1}{y}\right)\right] \exp(-iq_n y)$$

$$- \sum_n \lim_{\epsilon \to 0} A_n(\epsilon) \exp\left(-\frac{\pi \mathcal{Q}_n}{2\epsilon}\right) \left[\frac{2 \cos k}{\omega + vq_n - 2\cos(k - q_n)} \frac{1}{y^2} + O\left(\frac{1}{y^3}\right)\right] \exp(iq_n y). \quad (34b)$$

[Here we have used Eq. (25).] Matching Eq. (34a) to Eq. (31a) and Eq. (34b) to Eq. (31b) yields then $K_0 = 0$ and

$$\lim_{\epsilon \to 0} A_n(\epsilon) \exp\left(-\frac{\pi \mathcal{Q}_n}{2\epsilon}\right) = 0, \quad (35a)$$

$$\lim_{\epsilon \to 0} A_n^*(\epsilon) \exp\left(\frac{\pi \mathcal{Q}_n}{2\epsilon}\right) = K_n, \quad (35b)$$

for $n = 1, 2, \ldots$. We note that Eq. (35a) follows from Eq. (35b), while the latter equation can be written, symbolically, as

$$A_n(\epsilon) \to K_n^* \exp\left(-\frac{\pi \mathcal{Q}_n}{2\epsilon}\right) \quad \text{as } \epsilon \to 0. \quad (36)$$

Our subsequent efforts will focus on the evaluation of the constants K_n.

For k greater than $k_{\max}^{(1)}$ (approximately 0.22), there is only one radiation mode and therefore only one preexponential factor, K_1. For smaller k we note that the amplitude of the nth radiation mode, A_n, is a factor of $\exp\{\frac{\pi}{2\epsilon}(\mathcal{Q}_n - \mathcal{Q}_1)\}$ smaller than A_1, the amplitude of the first mode. Referring to Fig. 1, it is clear that for $n \geq 3$, the difference $\mathcal{Q}_n - \mathcal{Q}_1$ will be no smaller than π. As for the second mode, it becomes as sig-

nificant as the first one only when $k=O(\epsilon^2)$ in which case $(Q_2-Q_1)/\epsilon=O(1)$. But in our asymptotic expansion of Sec. II we assumed, implicitly, that k is of order 1 and so the case of $k=O(\epsilon^2)$ is beyond the scope of our current analysis. Therefore, for our purposes all the radiation modes with $n \geq 2$ (when they exist) will have negligible amplitudes compared to that of the first mode, provided K_1 is nonzero and ϵ is small. For this reason, we shall only attempt to evaluate K_1 in this paper.

E. Borel summability of the asymptotic series

Pomeau, Ramani, and Grammaticos [45] have shown that the radiation can be measured using the technique of Borel summation rather than by solving differential equations numerically, as in Segur and Kruskal's original approach. The method has been refined by (among others) Grimshaw and Joshi [46,47] and Tovbis *et al.* [48–51], who have applied it to difference equations. Most recently it has been applied to differential-difference equations in the context of moving kinks in ϕ^4 models [36]. This is the approach that we will be pursuing here.

Expressing $u(y)$ and $w(y)$ as Laplace transforms

$$u(y) = \int_\gamma U(p)e^{-py}dp \qquad (37a)$$

and

$$w(y) = \int_\gamma W(p)e^{-py}dp, \qquad (37b)$$

where γ is a contour extending from the origin to infinity in the complex p plane, the inner equations (27) are cast in the form of integral equations

$$f(p)U + \mu[f(p)U]*U*W + U*U*W = 0, \quad (38a)$$

$$f(-p)W + \mu[f(-p)W]*W*U + W*W*U = 0, \qquad (38b)$$

where

$$f(p) = (\cosh p - 1)\cos k - i(\sinh p - p)\sin k.$$

The asterisk $*$ denotes the convolution integral,

$$U(p)*W(p) = \int_0^p U(p-p_1)W(p_1)dp_1,$$

where the integration is performed from the origin to the point p on the complex plane, along the contour γ. In deriving Eqs. (38), we have made use of the convolution theorem for the Laplace transform of the form (37), where the integration is over a contour in the complex plane rather than a positive real axis. The theorem states that

$$u(y)w(y) = \int_\gamma [U(p)*W(p)]e^{-py}dp. \qquad (39)$$

The proof of this theorem is provided in Appendix A.

We choose the contour so that $\arg p \to \pi/2$ as $|p|\to\infty$ along γ. In this case we have $e^{-py}\to 0$ as $|p|\to\infty$ for all y

along any line $-\infty < \mathrm{Re}\, y < \infty$ with $\mathrm{Im}\, y < 0$. Therefore, the integrals in Eqs. (37) converge for all y along this line and any bounded $U(p)$ and $W(p)$.

The function $U(p)$ will have singularities at the points where $f(p)$ vanishes while the sum of the double-convolution terms in Eq. (38a) does not. Similarly, $W(p)$ will have a singularity wherever $f(-p)$ vanishes [while the sum of the double-convolution terms in Eq. (38b) does not]. Therefore, U and W may have singularities at the points where

$$\cosh p - 1 = \pm i \tan k\,(\sinh p - p), \qquad (40)$$

with the top and bottom signs referring to $U(p)$ and $W(p)$, respectively. The imaginary roots of Eq. (40) with the top sign are at $p=-iq_n$ and those of Eq. (40) with the bottom sign at $p=iq_n$, where q_n are the real roots of Eq. (30). (We remind the reader that all roots q_n are positive.) The point $p=0$ is not a singularity as both double-convolution terms in each line of Eqs. (38) vanish here. There is always at least one pure imaginary root of Eq. (40) (and *only* one if $k>k_{max}^{(1)}$, where $k_{max}^{(1)} \approx 0.22$).

In addition, there are infinitely many complex roots. The complex singularities of U [complex roots of the top-sign equation in Eq. (40)] are at the intersections of the curve given by

$$q = \frac{\cosh \kappa}{\sin k}\sqrt{1 - \sin^2 k\left(\frac{\kappa}{\sinh \kappa}\right)^2} - \cot k, \qquad (41a)$$

with the family of curves described by

$$q = k - \arcsin\left(\frac{\kappa}{\sinh \kappa}\sin k\right) + 2\pi n, \quad n = 1, 2, \ldots, \tag{41b}$$

and at the intersections of the curve

$$q = -\frac{\cosh \kappa}{\sin k}\sqrt{1 - \sin^2 k\left(\frac{\kappa}{\sinh \kappa}\right)^2} - \cot k, \qquad (42a)$$

with the family of curves described by

$$q = k + \arcsin\left(\frac{\kappa}{\sinh \kappa}\sin k\right) + \pi(2n + 1),$$

$$n = -2, -3, -4, \ldots. \tag{42b}$$

Here κ and q are the real and imaginary part of p: $p=\kappa+iq$. The curve (41a) looks like a parabola opened upwards, with the vertex at $\kappa=q=0$, and the curve (42a) like a parabola opened downwards, with the vertex at $\kappa=0$, $q=-2\cot k$. The curves (41b) and (42b), on the other hand, look like parabolas for small κ but then flatten out and approach horizontal straight lines as $\kappa\to\pm\infty$. [In compiling the list of these "flat" curves in Eqs. (41b) and (42b), we have taken into account that the curve (41b) with $n=0$ does not have any intersections with the parabola (41a) and the curve (42b) with $n=-1$ does not have any intersections with the parabola (42a).] As k is reduced, the vertex of the parabola (42a) moves down along the q axis; the intersections of this parabola with the "flat" curves (42b) approach, pairwise, the q axis. After col-

liding on the q axis, pairs of complex roots move away from each other along it. [The parabola (41a) does not move as k is reduced, but only steepens, which results in the singularities in the upper half-plane approaching the imaginary axis but not reaching it until $k=0$.] In a similar way, the complex singularities of $W(p)$ move onto the imaginary axis as k is decreased. In Sec. III E below we will use the fact that the distance from any complex singularity to the origin is larger than 2π; this follows from the observation that the closest points of the curves (41b) and (42b) to the origin are their intersections with the q axis. These are farther away than 2π from the origin.

In addition to singularities at $p=-iq_n$, the function $U(p)$ will have singularities at points $p=iq_n$, $n=1,2,\dots$. These are induced by the cubic terms in Eq. (38a); for instance, the singularity at $p=iq_1$ arises from the convolution of the term proportional to p in $U*U$ with the function W which has a singularity at $p=iq_1$. [That $U(p)$ has singularities at $p=iq_n$ can also be seen directly from Eq. (31a).] Similarly, the function $W(p)$ will have singularities at points $p=-iq_n$, $n=1,2,\dots$. By virtue of the nonlinear terms there will also be singularities at the "combination points" $i(\pm q_n \pm q_m)$, $i(\pm q_n \pm q_m \pm q_j)$, etc.

The formal inverse-power series (28), which we can write as

$$\hat{u}(y) = \sum_{\ell=0}^{\infty} \rho_\ell \frac{\ell!}{y^{\ell+1}}, \quad \hat{w}(y) = \sum_{\ell=0}^{\infty} \nu_\ell \frac{\ell!}{y^{\ell+1}}, \qquad (43)$$

result from the Laplace transformation of power series for $U(p)$ and $W(p)$:

$$U(p) = \sum_{\ell=0}^{\infty} \rho_\ell p^\ell, \quad W(p) = \sum_{\ell=0}^{\infty} \nu_\ell p^\ell. \qquad (44)$$

The series (44) converge in the disk of radius q_1, centered at the origin, and hence can be integrated term by term only over the portion of the contour γ which lies within that disk. However, by Watson's lemma, the remaining part of the contour makes an exponentially small contribution to the integral and the resulting series (43) are asymptotic as $y \to \infty$. The functions $u(y)$ and $w(y)$ defined by Eqs. (37) give the Borel sums of the series $\hat{u}(y)$ and $\hat{w}(y)$.

Consider now some horizontal line in the inner region; that is, let Im $y < 0$ be fixed and Re y vary from $-\infty$ to ∞. If the integration contour γ is chosen to lie in the first quadrant of the complex p plane, the functions $u(y)$ and $w(y)$ generated by Eqs. (37) will tend to zero as Re $y \to +\infty$ along this line. Similarly, if it is chosen to lie in the second quadrant, they will tend to zero as Re $y \to -\infty$. Suppose there were no singularities between two such contours; then the one could be continuously deformed to the other without any singularity crossings; i.e., they would generate the same solution which, therefore, would decay to zero at both infinities. [That is, the oscillatory tails in Eqs. (31) would have zero amplitudes, $K_n=0$.] In general, however, $U(p)$ and $W(p)$ have singularities both on and away from the imaginary axis. In order to minimize the number of singularities to be crossed in the deformation of one contour to the other, we choose the con-
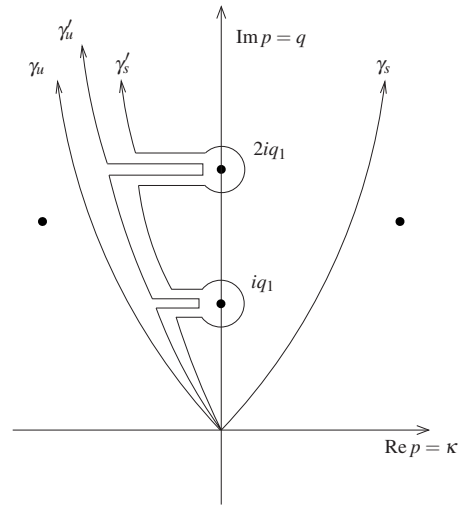

FIG. 2. The integration contours γ_s and γ_u used to generate the solutions (u_s, w_s) and (u_u, w_u), respectively, via Eqs. (37). The dots are singularities of $W(p)$. Shown is the situation where the linear dispersion relation (30) has only one real root, q_1.

tours to lie above all singularities with nonzero real part. (That this is possible, is shown in Appendix B.) Note also that the imaginary part of the singularity grows faster than its real part and hence arg p should tend to $\pi/2$ as $|p| \to \infty$ along γ; this was precisely our choice for the direction of the contours γ in the beginning of Sec. III E.

Let γ_s and γ_u be two contours chosen in this way, with γ_s lying in the first quadrant and γ_u in the second quadrant. The solutions $u(y)$ and $w(y)$ generated by Eqs. (37) with the contour γ_s will tend to zero as Re $y \to \infty$ (with Im $y < 0$ fixed). Hence they can be identified with solutions u_s and w_s obtained by the continuation of the outer solution ψ_s which has the same asymptotic behavior. Similarly, the solutions generated by Eqs. (37) with the contour γ_u coincide with solutions u_u and w_u—like u_u and w_u, the solutions generated by Eqs. (37) tend to zero as Re $y \to -\infty$ (with fixed Im $y < 0$).

Consider, first, solutions w_s and w_u. Since the contours γ_s and γ_u are separated by singularities of $W(p)$ on the positive imaginary axis, they cannot be continuously deformed to each other without singularity crossings and so the solution w_s does not coincide with w_u, unless the residue at the singularity happens to be zero. If we deform γ_s to γ_s' and γ_u to γ_u' as shown in Fig. 2, without crossing any singularities, then the only difference between the two contours is that γ_s' encircles the singularities, whereas γ_u' does not. Therefore, the difference $w_s - w_u$ can be deduced exclusively from the leading-order behavior of $W(p)$ near its singularities. There can be two contributions to this difference: the first arises from integrating around the poles and is a sum of residues, while the second arises if the singularity is a branch point.

To find the singularity structure of the function $W(p)$, we equate

$$w_s - w_u = \int_{\gamma_s'} W(p) e^{-py} dp - \int_{\gamma_u'} W(p) e^{-py} dp \qquad (45)$$

to the expansion (31b). The first term in Eq. (31b), $e^{-iq_n y}$, arises from the integration of a term $(2\pi i)^{-1}(p-iq_n)^{-1}$ in

$W(p)$. For such a term, the difference of the two integrals in Eq. (45) reduces to an integral around a circle centered on the point $p=iq_n$:

$$\frac{1}{2\pi i}\oint \frac{1}{p-iq_n}e^{-py}dp=\mathrm{res}\left\{\frac{e^{-py}}{p-iq_n},iq_n\right\}.$$

The term $y^{-m}e^{-iqy_n}$ in Eq. (31b), with $m=1,2,\ldots$, arises from the integration of a term

$$\frac{1}{2\pi i}\frac{(p-iq_n)^{m-1}}{(m-1)!}\ln(p-iq_n)$$

in $W(p)$. This time, $p=iq_n$ is a branch point. After going around this point along the circular part of γ_s', the logarithm increases by $2\pi i$ and the difference between the integrals in Eq. (45) is given by

$$\frac{1}{(m-1)!}\int_C (p-iq_n)^{m-1}e^{-py}dp=\frac{e^{-iq_ny}}{(m-1)!}\int_0^\infty z^{m-1}e^{-zy}dz,$$

where C is the part of γ_s' extending from $p=iq_n$ to infinity. This equals exactly $y^{-m}e^{-iq_ny}$.

Thus, in order to generate the full series (31b) we must have

$$W(p)=\frac{1}{2\pi i}\sum_n K_n\left[\frac{1}{p-iq_n}+\sum_{m=1}^\infty \frac{c_m^{(n)}}{(m-1)!}(p-iq_n)^{m-1}\right.$$
$$\left.\times\ln(p-iq_n)\right]+W_{\mathrm{reg}}(p),\qquad(46)$$

where W_{reg} denotes the part of W which is regular at $p=iq_n$, $n=1,2,\ldots$. By the same process, matching u_s-u_u to δu in Eq. (31a) yields

$$U(p)=\frac{1}{2\pi i}\sum_n K_n\sum_{m=1}^\infty \frac{d_m^{(n)}}{(m-1)!}(p-iq_n)^{m-1}\ln(p-iq_n)$$
$$+U_{\mathrm{reg}}(p).\qquad(47)$$

The solution to Eqs. (38) is nonunique; for instance, if $\{U(p),W(p)\}$ is a solution, then so is $\{e^{py_0+\zeta_0}U(p),e^{py_0-\zeta_0}W(p)\}$ with any complex y_0 and ζ_0. Also, if $\{U(p),W(p)\}$ is a solution, $\{W(-p),U(-p)\}$ is another one. We will impose the constraint

$$U(p)=W(-p);\qquad(48)$$

this constraint is obviously compatible with Eqs. (38). It is not difficult to see that the reduction (48) singles out a unique solution of Eqs. (38). The motivation for imposing the constraint (48) comes from the symmetry $\hat{u}(-y)=-\hat{w}(y)$ of the power-series solution of Eq. (27). Using this symmetry in Eq. (43), we get $\rho_\ell=(-1)^\ell\nu_\ell$ and then Eq. (44) implies Eq. (48).

In view of Eq. (48), the singularities of $U(p)$ in the upper half-plane are singularities of $W(p)$ in the lower half-plane, which fall within $W_{\mathrm{reg}}(p)$, and vice versa. Thus we have, finally,

$$W(p)=\frac{1}{2\pi i}\sum_n \frac{K_n}{p-iq_n}+\frac{1}{2\pi i}\sum_n K_n\sum_{m=1}^\infty \frac{1}{(m-1)!}$$
$$\times[c_m^{(n)}(p-iq_n)^{m-1}\ln(p-iq_n)$$
$$-(-1)^m d_m^{(n)}(p+iq_n)^{m-1}\ln(p+iq_n)]+\widetilde{W}_{\mathrm{reg}}(p),$$
$$(49)$$

where $\widetilde{W}_{\mathrm{reg}}(p)$ is regular at $p=\pm iq_n$. We also mention an equivalent representation for Eq. (49) which turns out to be computationally advantageous:

$$W(p)=\frac{1}{2\pi i}\sum_n K_n\sum_{m=0}^\infty D^{-m}\left[\frac{c_m^{(n)}}{p-iq_n}-\frac{(-1)^m d_m^{(n)}}{p+iq_n}\right]+\check{W}_{\mathrm{reg}}(p).$$
$$(50)$$

Here D^{-1} is an integral map:

$$D^{-1}f(p)\equiv\int_0^p f(p_1)dp_1;$$

the notation $D^{-m}f(p)$ should be understood as

$$D^{-m}f(p)\equiv\int_0^p dp_1\int_0^{p_1} dp_2\int_0^{p_2} dp_3\cdots\int_0^{p_{m-1}} dp_m f(p_m).$$

We have also introduced $c_0^{(n)}=1$ and $d_0^{(n)}=0$ for economy of notation. The only difference between Eqs. (49) and (50) is that the double-sum term on the right-hand side of Eq. (50) includes some terms which are regular at $p=\pm iq_n$, whereas in Eq. (49), all regular terms are contained in $\widetilde{W}_{\mathrm{reg}}(p)$.

The residues K_n at the poles of $W(p)$ are known as the Stokes constants. The leading-order Stokes constant K_1 can be related to the behavior of the coefficients in the power-series expansion of $W(p)$. Indeed, the coefficients in the power series (44) satisfy

$$\nu_\ell\to K_1\sum_{m=0}^\ell \frac{c_m^{(1)}+(-1)^\ell d_m^{(1)}}{2\pi q_1(iq_1)^{\ell-m}}\frac{(\ell-m)!}{\ell!}\quad\text{as }\ell\to\infty.\quad(51)$$

This is obtained by expanding the singular part of the expression (50) in powers of p. (Coefficients of the regular part become negligible in the limit $\ell\to\infty$ compared to those of the singular part.) Note that we have ignored singularities with nonzero real part and singularities on the imaginary axis other than at $p=\pm iq_1$. The reason is that all these singularities are farther away from the origin than the points $\pm iq_1$ (in particular all complex singularities are separated from the origin by a distance greater than 2π), and their contribution to ν_ℓ becomes vanishingly small as $\ell\to\infty$. We have also neglected singularities at the "combination points" because of their exponentially small residues. The coefficients ν_ℓ can be calculated numerically; once they are known, it follows from (51) that

$$K_1=2\pi q_1\lim_{\ell\to\infty}(iq_1)^\ell\nu_\ell\qquad(52)$$

(where we have recalled that $c_0^{(1)}=1$ and $d_0^{(1)}=0$).

We now turn to the numerical calculation of the coefficients ν_ℓ.

F. Recurrence relation

To make our forthcoming numerical procedure more robust, we normalize the coefficients in the power series (44) by writing

$$\nu_\ell = -i\frac{\delta_\ell}{(iq_1)^\ell}. \qquad (53)$$

Substituting the expansions (44) with Eq. (53) as well as the constraint (48) into either of equations (38) and equating coefficients of like powers of p yields the following recurrence relation for the numbers δ_n $(n \geq 0)$:

$$\sum_{m=0}^{n} \frac{q_1^m \delta_{n-m}}{(m+2)!} \mathcal{R}_m$$

$$= \frac{1}{(n+2)(n+1)} \sum_{m=0}^{n} \left[\delta_{n-m} + \mu \sum_{j=2}^{n-m} \frac{q_1^j \delta_{n-m-j}}{j!} \mathcal{R}_j \right]$$

$$\times \left(\sum_{j=0}^{m} (-1)^{m-j} \delta_{m-j} \delta_j \frac{j!(m-j)!}{m!} \right) \frac{m!(n-m)!}{n!}. \qquad (54)$$

Here

$$\mathcal{R}_m = \begin{cases} (-1)^{m/2} \cos k, & \text{for } m \text{ even,} \\ (-1)^{(m-1)/2} \sin k, & \text{for } m \text{ odd.} \end{cases}$$

Solving Eq. (54) with $n=0$ gives $\delta_0 = \sqrt{1-c^2}$. Thereafter it can be solved for each member of the sequence $\{\delta_n\}$ in terms of the preceding ones, and thus each δ_n can be calculated in turn. [Since all the coefficients in the recurrence relation (54) are real, the sequence $\{\delta_n\}$ turns out to be a sequence of real numbers.]

Once the sequence $\{\delta_n\}$ has been generated, expression (52) can be used to calculate the Stokes constant. We have

$$K_1 = -2\pi i q_1 \delta_\ell \qquad (55)$$

for sufficiently large ℓ. Unfortunately, the convergence of the sequence $\{\delta_n\}$ is slow and thus the above procedure is computationally expensive. The convergence can be accelerated by expanding Eq. (51) in powers of small $1/\ell$:

$$\delta_\ell = \frac{iK_1}{2\pi q_1} \left[1 + iq_1 \frac{c_1^{(1)}}{\ell} - q_1^2 \frac{c_2^{(1)} + (-1)^\ell d_2^{(1)}}{\ell^2} + O\left(\frac{1}{\ell^3}\right) \right],$$

whence

$$K_1 = -2\pi i q_1 \delta_\ell \left[1 - iq_1 \frac{c_1^{(1)}}{\ell} + q_1^2 \frac{c_2^{(1)} - (c_1^{(1)})^2 + (-1)^\ell d_2^{(1)}}{\ell^2} + O\left(\frac{1}{\ell^3}\right) \right]. \qquad (56)$$

According to Eq. (56), Eq. (55) gives K_1 with a relatively large error of order $1/\ell$. On the other hand, a two-term approximation
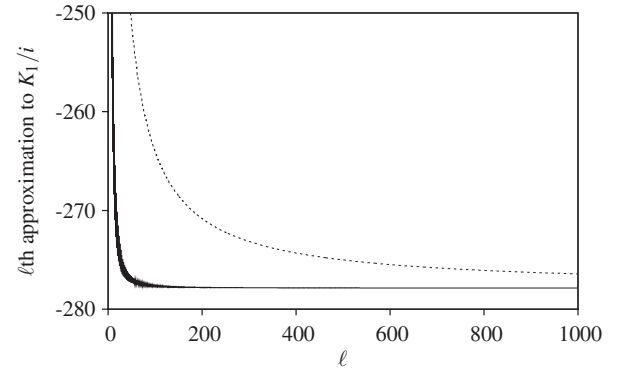

FIG. 3. Convergence of the sequence on the right-hand side of Eq. (55) (dashed line) and the "accelerated" sequence defined by the right-hand side of Eq. (57) (solid line). Shown are the ℓth approximations to the Stokes constant K_1 [the ℓth members of the sequences (55) and (57)] divided by i to get a real value. In this plot, $\mu=0$ and $k=0.5$.

$$K_1 = -2\pi i q_1 \delta_\ell \left(1 - iq_1 \frac{c_1^{(1)}}{\ell} \right) \qquad (57)$$

is correct to $O(1/\ell^2)$. More precisely, the relative error associated with the answer (57) is given by

$$\frac{\mathcal{E}}{K_1} = q_1^2 \frac{c_2^{(1)} - (c_1^{(1)})^2 + (-1)^\ell d_2^{(1)}}{\ell^2}. \qquad (58)$$

In our calculations, we set $\mathcal{E}/K_1 = 10^{-5}$. Since $c_1^{(1)}$, $c_2^{(1)}$, and $d_2^{(1)}$ are known constants [given by Eqs. (32a) and (32b)], Eq. (58) tells us what ℓ we should take—i.e., how many members of the sequence $\{\delta_n\}$ we should calculate in order to achieve the set accuracy. Figure 3 illustrates the convergence of the approximate values of K_1 calculated using Eqs. (55) and (57) as ℓ is increased. Note the drastic acceleration of convergence in the latter case.

Figure 4(a) shows the calculated Stokes constant as a function of k for various values of the saturation parameter μ. First of all, $K_1(k)$ does not have any zeros in the case of the cubic nonlinearity ($\mu=0$). This means that solitons of the cubic one-site discrete NLS equation [Eq. (2) with $\mu=0$] cannot propagate without losing energy to radiation. For $\mu = 3$ the Stokes constant does have a zero, but at a value of k smaller than $k_{\max}^{(1)}$ (where $k_{\max}^{(1)} \approx 0.22 = 0.07\pi$). Since higher radiation modes do exist in this range of k, there will still be radiation from the soliton—unless the "higher" Stokes constants $K_2(k)$, $K_3(k), \ldots$ happen to be zero at the same value of k. Finally, for $\mu=4$ the zero is seen to have moved just above $k_{\max}^{(1)}$ and for $\mu=6$ it has an even higher value. There are no $\mathcal{Q}_2, \mathcal{Q}_3, \ldots$ radiations for these k; hence, the zeros of $K_1(k)$ define the carrier wavenumbers at which the soliton "slides"—i.e., travels without emitting any radiation. Equation (17) then gives the corresponding sliding velocities, for each ϵ.

Figure 4(b) shows the Stokes constant $K_1(k)$ for higher values of the parameter μ. For $\mu=12$ a second zero of the Stokes constant has appeared, while for $\mu=25$, the function
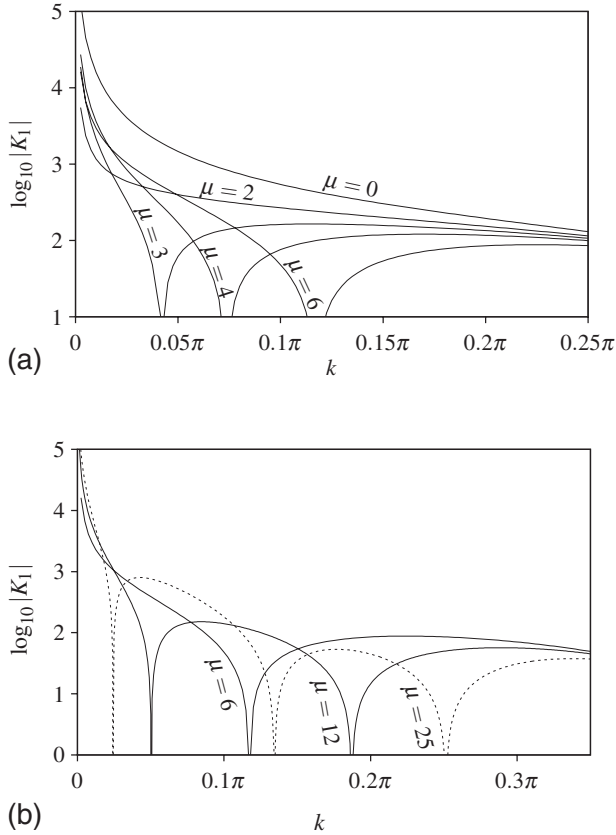
FIG. 4. The Stokes constant K_1 for various values of μ. Note the logarithmic scale on the vertical axis. The downward spikes extend all the way to $-\infty$; hence, each spike corresponds to a zero crossing. Each panel shows only a portion of the full range $0 \leq k \leq \pi/2$; there are no additional zero crossings in the part which is not shown.

$K_1(k)$ has three zeros. As μ is increased, the existing zeros move to larger values of k while new ones emerge at the origin of the k axis.

G. Radiation waves

For not very large $|X|$, the solution ψ_s is close to the localized pulse found by means of the perturbation expansion in Sec. II. As $X \to +\infty$, it tends to zero, by definition, while the $X \to -\infty$ asymptotic behavior is found from $\psi_s = \psi_u + \Psi$. Here the solution ψ_u decays to zero as $X \to -\infty$ and hence ψ_s approaches the oscillatory wave form Ψ given by Eqs. (24), (25), and (36):

$$\psi_s(X) \to \sum_n K_n^* e^{-\pi \mathcal{Q}_n/2\epsilon}$$
$$\times \left[1 + \epsilon \frac{4i \cos k \tan X}{2 \sin(k + \mathcal{Q}_n) - v} + O(\epsilon^2) \right] e^{i \mathcal{Q}_n X/\epsilon}$$

(59)

as $X \to -\infty$. Equation (59) describes a radiation background over which the soliton is superimposed. As we have explained, we can ignore all but the first term in the sum.

To determine whether the radiation is emitted by the soliton or being fed into it from outside sources, we consider a

harmonic solution $\psi = e^{i\mathcal{Q}X/\epsilon - i\Omega t}$ of the linearized equation (21); the corresponding dispersion relation is

$$\Omega(\mathcal{Q}) = -2 \cos(k + \mathcal{Q}) + \omega - \mathcal{Q}v.$$

The radiation background Ψ consists of harmonics with $\Omega = 0$ and $\mathcal{Q} = \mathcal{Q}_n$ where $\mathcal{Q}_n$ are roots of Eq. (18). The group velocities of these harmonic waves are given by

$$\Omega'(\mathcal{Q}_n) = 2 \sin(k + \mathcal{Q}_n) - v.$$

(60)

The $\mathcal{Q}_n$'s are zeros of the function $\Omega(\mathcal{Q})$, and the group velocities are the slopes of this function at its zeros; thus, the group velocities $\Omega'(\mathcal{Q}_1), \Omega'(\mathcal{Q}_2), \ldots$, have alternating signs. The first one, which is the only one that concerns us in this work, must be negative. Indeed, the value

$$\Omega(0) = -2 \cos k + \omega = 2 \cos k (\cosh \epsilon - 1)$$

is positive, and hence the slope of the function $\Omega(\mathcal{Q})$ as it crosses the $\mathcal{Q}$ axis at $\mathcal{Q}_1 > 0$ is negative. Therefore, the first radiation mode, extending to $-\infty$, carries energy *away* from the soliton.

The even-numbered radiation modes (where present) in our asymptotic solution (59) have positive group velocities and hence describe the flux of energy fed into the system at the left infinity. A more interesting situation is obviously the one with no incoming radiation; the corresponding solution is obtained by subtracting off the required multiple of the solution to the linearized equation—e.g., $e^{i\mathcal{Q}_2 X/\epsilon}$. One would then have a pulse leaving the odd modes in its wake and sending even modes ahead of it.

If the first Stokes constant $K_1(k)$ has a zero at some $k = k_1$ while $\mathcal{Q}_1$ is the only radiation mode available (as happens in our saturable model with μ greater than approximately 4), then according to Eq. (59), the radiation from the soliton with the carrier-wave wavenumber k_1 is suppressed completely.

IV. TIME EVOLUTION OF A RADIATING SOLITON

A. Amplitude–wavenumber dynamical system

To find the radiation-induced evolution of the traveling soliton, we use conserved quantities of the advance-delay equation associated with Eq. (2). In the reference frame moving at the soliton velocity v this equation reads

$$i\varphi_t + \varphi(x+1,t) + \varphi(x-1,t) - iv\varphi_x + \frac{2|\varphi|^2 \varphi}{1 + \mu|\varphi|^2} = 0.$$

(61)

The discrete variable $\phi_n(t)$ in Eq. (2) is related to the value of the continuous variable $\varphi(x,t)$ at the point $x = n - vt$: $\phi_n(t) = \varphi(n - vt, t)$. For future use, we also mention the relation between $\varphi(x,t)$ and the corresponding solution of Eq. (21):

$$\varphi(x,t) = \psi(X,t) e^{ik(x+vt) + i\omega t}.$$

(62)

We first consider the number of particles integral:

$$N = \int_a^b |\varphi|^2 dx.$$

Multiplying Eq. (61) by φ^*, subtracting the complex conjugate and integrating yields the rate of change of the integral N:

$$i\frac{dN}{dt} = \int_{a-1}^a (\varphi^+ \varphi^* - \text{c.c.})dx + \int_b^{b+1} (\varphi^- \varphi^* - \text{c.c.})dx + iv|\varphi|^2 \Big|_a^b.$$

$$(63)$$

In Eq. (63), $\varphi^\pm \equiv \varphi(x \pm 1, t)$ and c.c. stands for the complex conjugate of the immediately preceding term. The integration limits $a < 0$ and $b > 0$ are assumed to be large ($|a|, b \gg \epsilon^{-1}$) but finite; for example, one can take $a, b = O(\epsilon^{-2})$.

Consider the soliton moving with a positive velocity and leaving radiation in its wake. This configuration is described by the solution ψ_s of Eq. (21); the corresponding solution of Eq. (61) has the asymptotic behavior $\varphi_s \to 0$ as $x \to +\infty$. Substituting the leading-order expression (23) for the soliton's radiation tail into Eq. (62) yields the asymptotic behavior at the other infinity:

$$\varphi_s(x,t) \to \sum_n A_n[1 + O(\epsilon)]e^{i(k+\mathcal{Q}_n)x + i(\omega + kv)t} \text{ as } x \to -\infty.$$

$$(64)$$

Since, as we have explained above, the $\mathcal{Q}_1$ radiation is dominant, it is sufficient to keep only the $n=1$ term in (64).

Substituting (64) into (63) and evaluating the integral over the region $(a-1, a)$ in the soliton's wake, we obtain

$$\frac{dN}{dt} = |K_1|^2 e^{-\pi \mathcal{Q}_1/\epsilon} [2 \sin(k + \mathcal{Q}_1) - v],$$

$$(65)$$

where we have used Eq. (36). Note that $[2 \sin(k + \mathcal{Q}_1) - v]$ is the group velocity of the first radiation mode, $\Omega'(\mathcal{Q}_1)$, which, as we have established, is negative; hence, $\dot{N} \leq 0$.

We now turn to the momentum integral,

$$P = \frac{i}{2} \int_a^b (\varphi_x^* \varphi - \varphi_x \varphi^*)dx.$$

Multiplying Eq. (61) by φ_x^*, adding its complex conjugate, and integrating gives the rate equation

$$\frac{dP}{dt} = \int_{a-1}^a (\varphi^+ \varphi_x^* + \text{c.c.})dx - \int_b^{b+1} (\varphi^- \varphi_x^* + \text{c.c.})dx$$
$$+ \frac{i}{2}(\varphi \varphi_t^* - \varphi^* \varphi_t)\Big|_a^b - (\varphi^+)^* \varphi \Big|_{a-1}^b - (\varphi^-)^* \varphi \Big|_a^{b+1}$$
$$- \left[\frac{2}{\mu}|\varphi|^2 - \frac{2}{\mu^2} \ln(1 + \mu|\varphi|^2)\right]_a^b.$$

$$(66)$$

Evaluating the right-hand side of Eq. (66) similarly to the way we obtained Eq. (65) and substituting Eq. (18) for ω produces

$$\frac{dP}{dt} = |K_1|^2 e^{-\pi \mathcal{Q}_1/\epsilon}(k + \mathcal{Q}_1)[2 \sin(k + \mathcal{Q}_1) - v].$$

$$(67)$$

Using the leading-order term of the perturbative solution (13) and Eq. (62), we can express N and P via ϵ and k:

$$N = 2\epsilon \cos k + O(\epsilon^2),$$

$$P = 2k\epsilon \cos k + O(\epsilon^2).$$

In calculating N and P we had to integrate from $X = \epsilon a$ to $X = \epsilon b$. Since the integrands decay exponentially and since $a < 0$ and $b > 0$ were assumed to be much larger than ϵ^{-1} in absolute value, it was legitimate to replace these limits with $-\infty$ and ∞, respectively. The error introduced in this way is exponentially small in ϵ.

Taking time derivatives of N and P above and discarding ϵ^1 corrections to ϵ^0 terms, we deduce that

$$\dot{\epsilon} = \frac{\dot{N} + \tan k(\dot{P} - k\dot{N})}{2 \cos k},$$

$$\dot{k} = \frac{\dot{P} - k\dot{N}}{2\epsilon \cos k}.$$

Finally, substituting for $\dot{N}$ and $\dot{P}$ from Eqs. (65) and (67), we arrive at the dynamical system

$$\dot{\epsilon} = |K_1(k)|^2 e^{-\pi \mathcal{Q}_1/\epsilon} \Omega'(\mathcal{Q}_1)\frac{1 + \mathcal{Q}_1 \tan k}{2 \cos k}, \quad (68a)$$

$$\dot{k} = |K_1(k)|^2 e^{-\pi \mathcal{Q}_1/\epsilon} \Omega'(\mathcal{Q}_1)\frac{\mathcal{Q}_1}{2\epsilon \cos k}, \quad (68b)$$

where the group velocity $\Omega'(\mathcal{Q}_1) = 2 \sin(k + \mathcal{Q}_1) - v$, with $v = 2(\sinh \epsilon/\epsilon)\sin k$, and $\mathcal{Q}_1 = \mathcal{Q}_1(\epsilon, k)$ is the smallest root of Eq. (19).

B. Soliton's deceleration and sliding velocities

The vector field (68) is defined for $k \geq k_{\min}^{(1)}$, where $k_{\min}^{(1)}$ is the value of k for which the roots $\mathcal{Q}_1$ and $\mathcal{Q}_2$ merge in Fig. 1 (i.e., the smallest value of k for which the roots $\mathcal{Q}_1$ and $\mathcal{Q}_2$ still exist). When $k = k_{\min}^{(1)}$, the group velocity $\Omega'(\mathcal{Q}_1)$ becomes equal to zero; therefore, the equation $k = k_{\min}^{(1)}(\epsilon)$ defines a line of (nonisolated) fixed points of the system (68). Assume, first, that the saturation parameter μ is such that $K_1(k)$ does not vanish for any k. For $k > k_{\min}^{(1)}$, the factor $\Omega'(\mathcal{Q}_1)$ in Eq. (68b) is negative; since $\mathcal{Q}_1$ and $\cos k$ are positive for all $0 < k \leq \pi/2$, the derivative $\dot{k}$ satisfies $\dot{k} \leq 0$ for all times. Hence, all trajectories are flowing towards the line $k = k_{\min}^{(1)}(\epsilon)$ from above. It is worth noting that the derivative $\dot{\epsilon}$ is also negative and that the k axis is also a line of nonisolated fixed points. However, no trajectories will end there as follows from the equation

$$\frac{d\epsilon}{dk} = \epsilon \left[\tan k + \frac{1}{\mathcal{Q}_1(k, \epsilon)}\right],$$

which is a consequence of Eqs. (68a) and (68b).

Representative trajectories are plotted in Fig. 5(a). Since $k_{\min}^{(1)}(\epsilon) \approx \epsilon^2/4\pi$ is very small for small ϵ, the line $k = k_{\min}^{(1)}(\epsilon)$
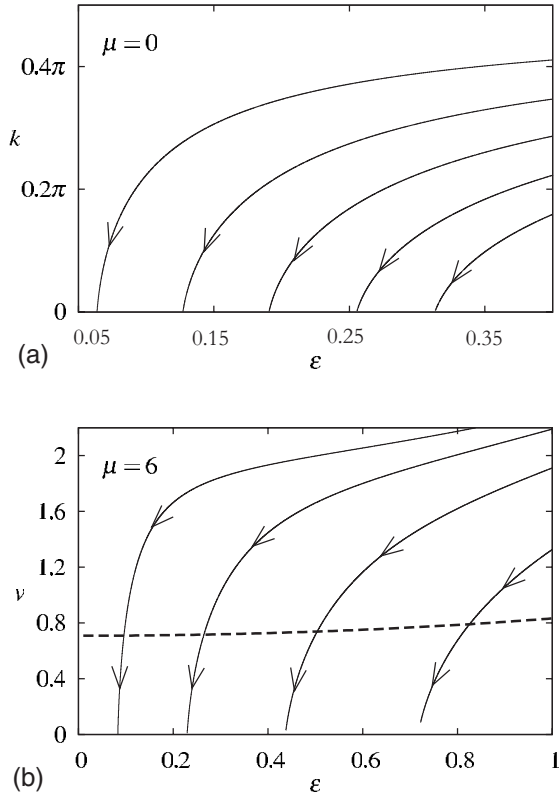
(a)

(b)

FIG. 5. The phase portrait of the system (68) in the case (a) where the Stokes constant $K_1(k)$ does not have zeros and (b) where $K_1(k)$ has one zero. In (b), the dashed line is the line of nonisolated fixed points $k=k_1$. Note that in (b), the phase portrait has been replotted on the (ϵ,v) plane; hence, the dashed line gives the value of the sliding velocity for each value of ϵ. In (a), $\mu=0$; in (b), $\mu=6$.

is practically indistinguishable from the horizontal axis. Therefore, we can assert that, to a good accuracy, $k\rightarrow0$ as $t\rightarrow\infty$. This means that the soliton stops moving—and stops decaying at the same time.

For k smaller than $k_{\min}^{(1)}$, the vector field (68) is undefined and we cannot use it to find out what happens to the soliton after k has reached $k_{\min}^{(1)}$. The reason for this is that the soliton stops radiating at the wavenumber $\mathcal{Q}_1$ as k drops below $k_{\min}^{(1)}$. In fact our analysis becomes invalid as soon as k becomes $O(\epsilon^2)$—i.e., even before k reaches $k_{\min}^{(1)}$—because we can no longer disregard the $n=2$ radiation here. At the qualitative level it is obvious, however, that the parameter k should continue to decay all the way to zero, in a cascade way. First, the $n=2$ radiation will become as intense as the $n=1$ mode when k approaches $\epsilon^2/4\pi$. Subsequently—i.e., for k smaller than $\epsilon^2/4\pi$—the $n=3$ harmonic will replace the radiation with the wavenumbers $\mathcal{Q}_1$ and $\mathcal{Q}_2$ as a dominant mode. The $n=4$ mode will become equally intense near $k=k_{\min}^{(2)}\approx\epsilon^2/8\pi$; as k drops below $\epsilon^2/8\pi$, both $\mathcal{Q}_3$ and $\mathcal{Q}_4$ will cede to $\mathcal{Q}_5$ and so on.

If μ is such that the Stokes constant $K_1(k)$ vanishes at one or more values of k, the system has one or more lines of nonisolated fixed points, $k=k_i$. The corresponding values of v, $v=v_i(\epsilon)\equiv2(\sinh\epsilon/\epsilon)\sin k_i$, define the *sliding* velocities of the soliton—i.e., velocities at which the soliton moves with-
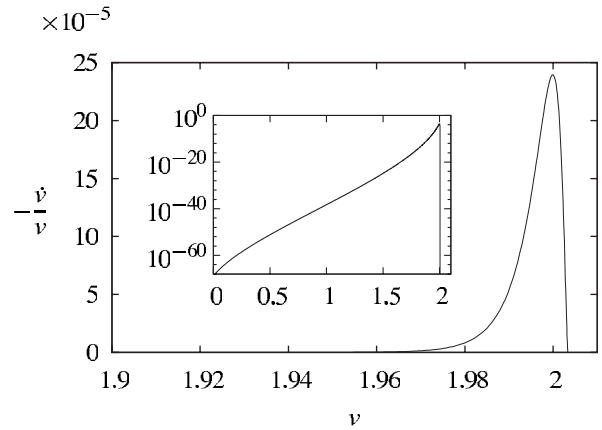

FIG. 6. The soliton's decay rate as a function of its velocity, for fixed $\epsilon=0.1$. (Here $\mu=0$.) In the inset, the same curve is replotted using a logarithmic scale on the vertical axis.

out radiative friction. One such velocity is shown by the dashed line in Fig. 5(b). The fixed points (ϵ,k_i) are semi-stable; for k above k_i, the flow is towards the line $k=k_i$, but when k is below k_i, the flow is directed away from this straight line [see Fig. 5(b)]. Since both $\dot{\epsilon}$ and $\dot{k}$ are negative, the soliton's velocity $v=2(\sinh\epsilon/\epsilon)\sin k$ will generally be decreasing—until it hits the nearest underlying sliding velocity v_i and locks on to it. The ensuing sliding motion will be unstable; a small perturbation will be sufficient to take the soliton out of the sliding regime after which it will resume its radiative deceleration. However, since $\dot{k}$ is proportional to the *square* of the Stokes constant and not to $K_1(k)$ itself, small perturbations δk will be growing linearly, not exponentially, in t. As a result, the soliton may spend a fairly long time sliding at the velocity v_i. It is therefore not unreasonable to classify this sliding motion as *metastable*.

We conclude that the soliton becomes pinned (i.e., $k\rightarrow0$ and so $v\rightarrow0$) before it has decayed fully (i.e., before the amplitude ϵ has decreased to zero). The exponential dependence of $\dot{\epsilon}$ and $\dot{k}$ on $1/\epsilon$ implies that tall, narrow pulses will be pinned very quickly while short, broad ones will travel for a very long time before they have slowed appreciably. Next, if μ is such that there is one or more sliding velocity available in the system, and if the soliton is initially moving faster than some of these, its deceleration will be interrupted by long periods of undamped motion at the corresponding sliding velocities.

It is worth reemphasizing here that if the amplitude ϵ is small, then even if the soliton is *not* sliding, its deceleration will be so slow that it will spend an exponentially long time traveling with virtually unchanged amplitude and speed. The deceleration rate $-\dot{v}/v$ is shown in Fig. 6 as a function of the soliton's velocity v for fixed amplitude ϵ. Note that the decay rate drops, exponentially, as the velocity is decreased; this drop is due to the exponential factor $e^{-\pi\mathcal{Q}_1/\epsilon}$ in Eq. (68). As the velocity v (and hence the wavenumber k) decreases, the root $\mathcal{Q}_1(\epsilon,k)$ grows towards the limit value of approximately 2π (see Fig. 1). This variation in $\mathcal{Q}_1$ is amplified by the division by small ϵ and exponentiation in $e^{-\pi\mathcal{Q}_1/\epsilon}$.

V. CONCLUDING REMARKS

A. Summary

In this paper, we have constructed the moving discrete soliton of the saturable NLS Eq. (2) as an asymptotic expansion in powers of its amplitude. The saturable nonlinearity includes the cubic NLS as a particular case (for which $\mu = 0$). Our perturbation procedure is a variant of the Lindstedt-Poincaré technique where corrections to the parameters of the solution are calculated along with the calculation of the solution itself. Although the resulting asymptotic series (13) for the soliton is generally not convergent, the associated expansions for its frequency and velocity sum up to exact explicit expressions (17).

From the divergence of the asymptotic series (13) it follows, in particular, that the traveling discrete soliton does not decay to zero at least at one of the two infinities. Instead, the soliton approaches, as $X \to \infty$ or $X \to -\infty$, an oscillatory resonant background (23) where the amplitudes A_n of its constituent harmonic waves lie beyond all orders of ϵ. For the soliton moving with a positive velocity and approaching zero as $X \to \infty$, the oscillatory background at the left infinity represents the Cherenkov radiation left in the soliton's wake. To evaluate the amplitudes of the harmonic waves arising as $X \to -\infty$, we have continued the radiating soliton into the complex plane, where it exhibits singularities. We then matched the asymptotic expansion (34) of the background near the lowest singularity on the imaginary X axis to the far-field asymptotic expansion (31) of the background solution of the "inner" equation—i.e., of the advance-delay equation "zoomed in" on this singularity. The asymptotic expansions here are in inverse powers of the zoomed variable, y. The amplitudes of the radiation waves were found to be exponentially small in ϵ, with the preexponential factors (the so-called Stokes constants) being dependent only on the soliton's carrier-wave wavenumber. Representing solutions to the inner equation as Borel sums of their asymptotic expansions, the Stokes constants can be related to the expansion coefficients; we have calculated these coefficients numerically, using algebraic recurrence relations.

The upshot of the calculation of the leading Stokes constant K_1 is that in the case of the cubic nonlinearity (i.e., for $\mu = 0$), $K_1(k)$ does not vanish for any k. This means that the cubic discrete soliton cannot "slide"—i.e., cannot move without radiative friction. The saturable solitons, on the other hand, *can* slide—provided the saturation parameter μ is large enough. This is because, for a sufficiently large μ, the Stokes constant $K_1(k)$ is found to have one or more zeros $k_1, k_2, \ldots$. Since the soliton with wavenumber $k > 0.22$ can have no higher-order resonances, those zeros which satisfy $k_i > 0.22$ do define the wavenumbers at which sliding motion occurs. For each value of the soliton's amplitude ϵ, the formula (17) then gives the sliding velocities $v(k_i, \epsilon)$.

The calculation of asymptotics beyond all orders is useful not only for determining the sliding velocities. Knowing the radiation amplitudes has allowed us to derive a two-dimensional dynamical system (68) for the soliton's parameters. Trajectories of this dynamical system describe the evolution of the soliton traveling at a generic speed. The evolution turns out to be simple: If μ is such that the Stokes constant $K_1(k)$ does not vanish anywhere in the region $k > 0.22$, the soliton decelerates, although very slowly. Eventually it becomes pinned to the lattice with a decreased but finite amplitude. However, if μ is such that there are sliding velocities in the system and if the soliton starts its motion with the velocity higher than some of these, then, although it will finally become pinned to the lattice, its deceleration will be interrupted by long periods of metastable sliding motion at these isolated velocities.

B. Concluding remarks

It is interesting to tie up the above results with our previous work on exceptional discretizations of the ϕ^4 model [36]. In that case we discovered that for some exceptional models (in which the stationary soliton possesses an effective translational symmetry), sliding velocities, at which the radiation disappears, do exist. The fact that all these models involve a complicated nonlocal discretization of the nonlinearity leads one to wonder whether the nonlinearity *has* to be discretized nonlocally in order for sliding solitons to exist. This question is answered—negatively—by our present work which gives a counterexample of a simple, local, and physically motivated nonlinearity supporting sliding solitons.

A remaining open issue is whether exceptionality of the system is a prerequisite for the existence of sliding solitary waves. Indeed, we have yet to encounter a nonexceptional discrete system permitting sliding motion.

We conclude this section by placing our results in the context of earlier studies of discrete solitons.

Moving solitons in the cubic DNLS equation have previously been studied by Ablowitz, Musslimani, and Biondini [13] (among others), using a numerical technique based on discrete Fourier transforms as well as perturbation expansions for small velocities. As we have done, these authors suggest that sliding (radiationless) solitons may not exist. They also observe, with the aid of numerical simulations, that strongly localized pulses are pinned quickly to the lattice, while broader ones are more mobile—results which are in agreement with ours.

Feddersen and co-workers [7,8] have studied the bifurcation of periodic traveling waves from constant solutions in the cubic DNLS equation, using numerical path-following techniques. They find that the paths terminate when the soliton's amplitude reaches a certain limit value, and in the light of our results it seems likely that this is the point at which the radiation becomes large enough to have an effect on the numerics.

Solitary waves which decay to constant values at the spatial infinities, despite the fact that the generic asymptotic behavior in the underlying model is oscillatory, are commonly referred to as embedded solitons. An example is given by the sliding solitons reported in this paper as well as the sliding kinks of [36]; both types of solitary waves propagate without exciting the resonant background oscillations. Embedded solitons have been studied for some time in continuous systems [52], but their history in lattice equations is younger. Recently, Malomed and co-workers have consid-

ered certain lattice equations with next-to-nearest-neighbor couplings and shown (by means of explicit solutions) that both stationary [53] and moving [54] embedded solitons exist. Stationary embedded solitons in discrete waveguide arrays have also been analyzed by Yagasaki, Champneys, and Malomed [55].

Finally, while preparing the revised version of this paper, we learned that Melvin *et al.* have obtained results very similar to ours. Using a combination of intuitive arguments and numerical computations, they have found sliding solitons for certain values of the parameters of a saturable DNLS model [56].

APPENDIX A: CONVOLUTION THEOREM FOR THE LAPLACE TRANSFORM IN THE COMPLEX PLANE

This appendix deals with the convolution property of the modified Laplace transform of the form (37), where the integration is along an infinite contour in the complex plane rather than the positive real axis. In the context of asymptotics beyond all orders, this transform was pioneered by Grimshaw and Joshi [46]. Since no proof of the convolution result (39) is available in the literature and since it requires a nontrivial property (concavity) of the integration contour, we produce such a proof here.

We wish to show that

$$\int_{\gamma} e^{-pz}F(p)dp \int_{\gamma} e^{-p'z}G(p')dp'$$
$$= \int_{\gamma} e^{-pz}\left[\int_{0}^{p} F(p_1)G(p-p_1)dp_1\right]dp, \qquad (A1)$$

where $\int_{0}^{p}$ stands for an integral along the curve γ from the origin to the point p on that curve. We assume that the curve γ extends from the origin to infinity on the complex plane, lies in its first quadrant (Re $p > 0$, Im $p > 0$), is described as a graph of a single-valued function Im $p = f(\text{Re } p)$ (i.e., never turns back on itself), and is concave-up everywhere:

$$\frac{d^2f}{d(\text{Re } p)^2} > 0 \quad \text{for } p \text{ on } \gamma.$$

We also assume that the function $G(p)$ is analytic in the region between the contour γ and the imaginary axis.

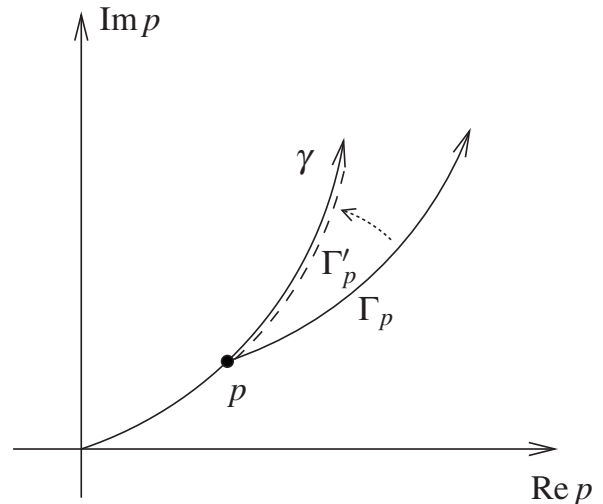We begin by writing the left-hand side of Eq. (A1) as

FIG. 7. Deformation of the integration contour Γ_p to Γ'_p.

$$\int_{\gamma}\int_{\gamma} e^{-(p+p')z}F(p)G(p')dp'dp$$
$$= \int_{\gamma} F(p)\left[\int_{\Gamma_p} e^{-rz}G(r-p)dr\right]dp, \qquad (A2)$$

where $r = p' + p$. The curve Γ_p is the path traced out by r as p' traces out the curve γ, for a given p (which also lies on γ)—this is depicted in Fig. 7. The path Γ_p is the same as the path γ but translated from the origin to the point p.

For each given p we deform the path Γ_p so that it now lies on γ, still starting at the point p. We call this deformed path Γ'_p. The point $r - p = p'$, which lay on the path γ before the deformation, will now move inside the region bounded by γ (i.e., the region to the left of γ), since all points on Γ'_p lie inside the region bounded by Γ_p. This follows from the fact that the path Γ_p is concave-up. The point $r - p$ will, however, stay to the right of the imaginary axis, since after the deformation, all points r on Γ'_p lie to the right of the point p. This follows from the fact that the curve γ never turns back on itself. Since $G(p')$ is analytic for all p' between the imaginary axis and γ, the value of the integral (A2) will not be affected by the deformation. [In the particular case of the functions $U(p)$ and $W(p)$ considered in Sec. III E, we have deliberately chosen the contours of integration so that the analyticity condition is satisfied.]

After the deformation, both integrals in Eq. (A2) follow the path γ, with the inner one starting at the point p. By parametrizing the path γ it is now straightforward to change the order of integration and end up with the desired result (A1).

The argument holds, with the obvious modifications, for paths in the second quadrant.

APPENDIX B: PROOF THAT SINGULARITIES DO NOT ACCUMULATE TO THE IMAGINARY AXIS

The roots of Eq. (40) with the top and bottom signs give singularities of $U(p)$ and $W(p)$, respectively. Our aim here is

to show that the integration contours γ_u and γ_s in Sec. III E can be chosen to lie above all the complex singularities—i.e., that singularities of $U(p)$ and $W(p)$ do not accumulate to the imaginary axis.

The roots of Eq. (40) are zeros of the functions $F(\pm p)$, where

$$F(p) \equiv \cosh p - 1 - i \tan k (\sinh p - p). \qquad (B1)$$

The imaginary zeros of $F(p)$ are at $p = -iq_n$, where q_n are the real roots of Eq. (30). We let N denote the number of these imaginary zeros; for $k \neq 0$, N is finite. We recall that all q_n are positive; hence, all N imaginary zeros of $F(p)$ are on the negative imaginary axis and all N zeros of $F(-p)$ on the positive imaginary axis.

Let κ and q be the real and imaginary part of p: $p = \kappa + iq$. We let $\mathcal{D}$ denote the rectangular region in the complex-p plane bounded by the vertical lines $\kappa = \pm \varepsilon$ and horizontal lines $q = \varepsilon^{1/2}$ and $q = Q$, where ε is small and Q is large enough for the region to contain all N zeros of $F(-p)$ on the positive imaginary axis. By the argument principle, the total number of (complex) zeros of the function $F(-p)$ in the region $\mathcal{D}$ is given by $(2\pi)^{-1}$ times the variation of its argument (i.e., its phase) along the boundary of $\mathcal{D}$. In a similar way, one may count the number of zeros of the function $F(p)$ in $\mathcal{D}$.

We have

$$\tan \arg F(\pm p) = \frac{\sinh \kappa \sin q \mp \tan k (\sinh \kappa \cos q - \kappa)}{\cosh \kappa \cos q - 1 \pm \tan k (\cosh \kappa \sin q - q)}.$$

Points on the vertical line $\kappa = \varepsilon$ satisfy

$$\tan \arg F(\pm p) \approx -\varepsilon \frac{d}{dq} \ln |1 - \cos q \pm \tan k (q - \sin q)|. \qquad (B2)$$

Consider, first, the case of the bottom sign in Eq. (B2). The expression between the bars in (B2) crosses through zero N times as the line $\kappa = \varepsilon$ is traced out. Each time zero is crossed, the logarithmic derivative in (B2) jumps from $-\infty$ to $+\infty$ and the argument of $F(-p)$ increases by π as we move from one crossing to the next one. The net increase of the argument as the line $\kappa = \varepsilon$ is traversed from its bottom to the top is $N\pi$. In the case of the top sign in (B2), on the other hand, the expression in $|\cdots|$ never crosses through zero and hence the total increment of the argument of $F(p)$ is zero.

As we move along the vertical line $\kappa = -\varepsilon$ from top to bottom, the argument of $F(-p)$ increases by another $N\pi$ while the argument of $F(p)$ does not acquire any increment. Since there are no zero crossings on the horizontal segments, the net change of the argument of $F(-p)$ along the boundary of $\mathcal{D}$ is $2N\pi$ while the total increment of $\arg F(p)$ is zero. Therefore $F(-p)$ has only N zeros in the region $\mathcal{D}$ (and they all lie on the imaginary axis) while the function $F(p)$ has no zeros in $\mathcal{D}$. This implies that complex singularities of $U(p)$ and $W(p)$ cannot accumulate to the positive imaginary axis.

[1] O. Braun and Yu. S. Kivshar, Phys. Rep. **306**, 1 (1998).
[2] D. Hennig and G. P. Tsironis, Phys. Rep. **307**, 333 (1999).
[3] A. Scott, *Nonlinear Science: Emergence and dynamics of coherent structures* (Oxford University Press, Oxford 1999).
[4] D. N. Christodoulides, F. Lederer, and Y. Silberberg, Nature (London) **424**, 817 (2003).
[5] D. K. Campbell, S. Flach, and Yu. S. Kivshar, Phys. Today **57**(1), 43 (2004).
[6] A. Trombettoni and A. Smerzi, Phys. Rev. Lett. **86**, 2353 (2001).
[7] H. Feddersen, in *Nonlinear Coherent Structures in Physics and Biology—Proceedings of the 7th Interdisciplinary Workshop, Dijon, France, 1991*, edited by M. Remoissenet and M. Peyrard, *Lecture Notes in Physics*, Vol. 393 (Springer, Berlin, 1991), pp. 159–167.
[8] D. B. Duncan, J. C. Eilbeck, H. Feddersen, and J. A. D. Wattis, Physica D **68**, 1 (1993).
[9] S. Flach and C. R. Willis, Phys. Rep. **295**, 181 (1998).
[10] S. Flach and K. Kladko, Physica D **127**, 61 (1999).
[11] S. Flach, Y. Zolotaryuk, and K. Kladko, Phys. Rev. E **59**, 6105 (1999).
[12] P. G. Kevrekidis, K. Ø. Rasmussen, and A. R. Bishop, Int. J. Mod. Phys. B **15**, 2833 (2001).
[13] M. J. Ablowitz, Z. H. Musslimani, and G. Biondini, Phys. Rev. E **65**, 026602 (2002).
[14] K. Kundu, J. Phys. A **35**, 8109 (2002).
[15] J. C. Eilbeck and M. Johansson, in *Proceedings of the Third Conference on Localization and Energy Transfer in Nonlinear Systems, San Lorenzo de El Escorial, Madrid, Spain, 2002* (World Scientific, Singapore, 2003), pp. 44–67.
[16] I. E. Papacharalampous, P. G. Kevrekidis, B. A. Malomed, and D. J. Frantzeskakis, Phys. Rev. E **68**, 046604 (2003).
[17] S. V. Dmitriev, P. G. Kevrekidis, B. A. Malomed, and D. J. Frantzeskakis, Phys. Rev. E **68**, 056603 (2003).
[18] D. E. Pelinovsky and V. M. Rothos, Physica D **202**, 16 (2005).
[19] J. Cuevas, B. A. Malomed, and P. G. Kevrekidis, Phys. Rev. E **71**, 066614 (2005).
[20] J. Gómez-Gardeñez, F. Falo, and L. M. Floría, Phys. Lett. A **332**, 213 (2004).
[21] J. Gómez-Gardeñez, L. M. Floría, M. Peyrard, and A. R. Bishop, Chaos **14**, 1130 (2004).
[22] N. K. Efremidis, S. Sears, D. N. Christodoulides, J. W. Fleischer, and M. Segev, Phys. Rev. E **66**, 046602 (2002).
[23] J. W. Fleischer, T. Carmon, M. Segev, N. K. Efremidis, and D. N. Christodoulides, Phys. Rev. Lett. **90**, 023902 (2003).
[24] F. Chen, C. E. Rüter, D. Runde, D. Kip, V. Shandarov, O. Manela, and M. Segev, Opt. Express **13**, 4314 (2005).
[25] J. W. Fleischer, M. Segev, N. K. Efremidis, and D. N. Christodoulides, Nature (London) **422**, 147 (2003).
[26] L. Hadžievski, A. Maluckov, M. Stepić, and D. Kip, Phys. Rev. Lett. **93**, 033901 (2004).
[27] M. Stepić, D. Kip, L. Hadžievski, and A. Maluckov, Phys. Rev. E **69**, 066618 (2004).
[28] J. Cuevas and J. C. Eilbeck, Phys. Lett. A **358**, 15 (2006).

[29] R. A. Vicencio and M. Johansson, Phys. Rev. E **73**, 046602 (2006).

[30] S. Gatz and J. Herrmann, J. Opt. Soc. Am. B **8**, 2296 (1991).

[31] S. Gatz and J. Herrmann, Opt. Lett. **17**, 484 (1992).

[32] V. Tikhonenko, J. Christou, and B. Luther-Davies, Phys. Rev. Lett. **76**, 2698 (1996).

[33] F. Vidal and T. W. Johnston, Phys. Rev. E **55**, 3571 (1997).

[34] A. Khare, K. Ø. Rasmussen, M. R. Samuelsen, and A. Saxena, J. Phys. A **38**, 807 (2005).

[35] I. V. Barashenkov, O. F. Oxtoby, and D. E. Pelinovsky, Phys. Rev. E **72**, 035602(R) (2005).

[36] O. F. Oxtoby, D. E. Pelinovsky, and I. V. Barashenkov, Nonlinearity **19**, 217 (2006).

[37] V. O. Vinetskii and N. V. Kukhtarev, Sov. Phys. Solid State **16**, 2414 (1975).

[38] See, e.g., A. H. Nayfeh and D. T. Mook, *Nonlinear Oscillations* (Wiley, New York, 1979); D. W. Jordan and P. Smith, *Nonlinear Ordinary Differential Equations* (Oxford University Press, Oxford, 1999).

[39] M. J. Ablowitz and J. F. Ladik, Stud. Appl. Math. **55**, 213 (1976); J. Math. Phys. **17**, 10011 (1976).

[40] E. W. Laedke, O. Kluth, and K. H. Spatschek, Phys. Rev. E **54**, 4299 (1996).

[41] D. E. Pelinovsky, Nonlinearity **19**, 2695 (2006).

[42] V. M. Eleonksii, N. E. Kulagin, N. S. Novozhilova, and V. P. Silin, Teor. Mat. Fiz. **60**, 395 (1984).

[43] H. Segur and M. D. Kruskal, Phys. Rev. Lett. **58**, 747 (1987).

[44] M. D. Kruskal and H. Segur, Stud. Appl. Math. **85**, 129 (1991).

[45] Y. Pomeau, A. Ramani, and B. Grammaticos, Physica D **31**, 127 (1988).

[46] R. H. J. Grimshaw and N. Joshi, SIAM J. Appl. Math. **55**, 124 (1995).

[47] R. H. J. Grimshaw, Stud. Appl. Math. **94**, 257 (1995).

[48] A. Tovbis, M. Tsuchiya, and C. Jaffé, Chaos **8**, 665 (1998).

[49] A. Tovbis, Contemp. Math. **255**, 199 (2000).

[50] A. Tovbis, Stud. Appl. Math. **104**, 353 (2000).

[51] A. Tovbis and D. Pelinovsky, Nonlinearity **19**, 2277 (2006).

[52] J. Fujioka, A. Espinosa-Cerón, and R. F. Rodríguez, Rev. Mex. Fis. **52**, 6 (2006).

[53] S. González-Pérez-Sandi, J. Fujioka, and B. A. Malomed, Physica D **197**, 86 (2004).

[54] B. A. Malomed, J. Fujioka, A. Espinosa-Cerón, R. F. Rodríguez, and S. González, Chaos **16**, 013112 (2006).

[55] K. Yagasaki, A. R. Champneys, and B. A. Malomed, Nonlinearity **18**, 2591 (2005).

[56] T. R. O. Melvin, A. R. Champneys, P. G. Kevrekidis, and J. Cuevas, Phys. Rev. Lett. **97**, 124101 (2006).